Impact of loss of NF-κB1, NF-κB2 or c-REL on SLE-like Autoimmune Disease and Lymphadenopathy in *Fas*$^{lpr/lpr}$ Mutant Mice

Jun T Low[1,2], Peter Hughes[3], Ann Lin[1], Ulrich Siebenlist[4], Reema Jain[1,2], Kelvin Yaprianto[1,2,*], Daniel H D Gray[1,2], Steve Gerondakis[5], Andreas Strasser[1,2], Lorraine A O'Reilly[1,2]

[1] The Walter and Eliza Hall Institute of Medical Research, Parkville, Victoria 3052, Australia

[2] Department of Medical Biology, The University of Melbourne, Parkville, Victoria 3052, Australia

[3] Department of Nephrology, The Royal Melbourne Hospital, Parkville, Victoria 3052, Australia

[4] Laboratory of Molecular Immunology, National Institute of Allergy and Infectious Diseases, NIH, Bethesda, MD USA

[5] Department of Biochemistry and Molecular Biology, Monash University, Clayton, Victoria 3800, Australia

* Current address, Stem Cell Division, Stem Cell and Cancer Institute, PT Kalbe Farma Tbk, Pulo Mas, Jakarta 13210, Indonesia

Running title: Role of NF-κB in mutant *Fas* autoimmune disease

Key words: autoimmunity, SLE, FAS, FASL, NF-κB, glomerulonephritis, dermatitis

Abbreviations: SLE: systemic lupus erythematosus; ANA: anti-nuclear antibodies; GN: glomerulonephritis; *Fas*$^{lpr/lpr}$: mice homozygous for the lymphoproliferation inducing spontaneous mutation

The authors declare no conflict of interest.

Address for correspondence
Dr Lorraine A. O' Reilly
The Walter and Eliza Hall Institute of Medical Research
1G Royal Parade
Parkville, Victoria 3052
Australia
Tel: (61-3) 9345 2499
Fax: (61-3) 9347 0852
Email: oreilly@wehi.edu.au

ABSTRACT

Defects in apoptosis can cause autoimmune disease. Loss-of-function mutations in the "death receptor", FAS, impair the deletion of auto-reactive lymphocytes in the periphery, leading to progressive lymphadenopathy and systemic lupus erythematosus (SLE)-like autoimmune disease in mice (*Fas*$^{lpr/lpr}$) and humans. The REL/NF-κB transcription factors regulate a broad range of immune effector functions and are also implicated in various autoimmune diseases. We generated compound mutant mice to investigate the individual functions of the NF-κB family members NF-κB1, NF-κB2 and c-REL in the various autoimmune pathologies of *Fas*$^{lpr/lpr}$ mutant mice. We show that loss of each of these transcription factors resulted in amelioration of many classical features of autoimmune disease, including hypergammaglobulinaemia, anti-nuclear autoantibodies (ANA) and autoantibodies against tissue-specific antigens. Remarkably, only c-REL-deficiency substantially reduced immune complex mediated glomerulonephritis and extended the lifespan of *Fas*$^{lpr/lpr}$ mice. Interestingly, compared to the *Fas*$^{lpr/lpr}$ animals, *Fas*$^{lpr/lpr}$*nfkb2*$^{-/-}$ mice presented with a dramatic acceleration and augmentation of lymphadenopathy that was accompanied by severe lung pathology due to extensive lymphocytic infiltration. The *Fas*$^{lpr/lpr}$*nfkb1*$^{-/-}$ mice exhibited the combined pathologies caused by defects in FAS-mediated apoptosis and premature aging due to loss of NF-κB1. These findings demonstrate that different NF-κB family members exert distinct roles in the development of the diverse autoimmune and lympho-proliferative pathologies that arise in *Fas*$^{lpr/lpr}$ mice and suggest that pharmacological targeting of c-REL should be considered as a strategy for therapeutic intervention in autoimmune diseases.

INTRODUCTION

Systemic Lupus Erythematosus (SLE) is a systemic autoimmune disease that affects approximately three million people worldwide. [1] The disease is characterised by dysregulated humoral, cellular and innate immune responses. Although milder forms of SLE (and certain other autoimmune diseases) can be controlled with immunosuppressive drugs, the chronic inflammation and tissue damage, particularly to the kidney resulting in lupus nephritis, is a major cause of morbidity and mortality. [1] Severe autoimmune kidney disease requiring dialysis or transplantation occurs in 10-30% of SLE patients. [1] Current therapeutic options are not focused on specific molecular targets and have many side effects leading to substantial complications. For example, the immune suppression resulting from several currently used therapeutics causes increased susceptibility to infection and certain cancers (e.g. EBV associated B cell lymphoma). [2] Hence, there is a need to identify molecular targets for novel therapies that improve the treatment of SLE and related autoimmune diseases.

Autoimmune diseases arise due to breakdown of immunological tolerance resulting in potently destructive immune responses against self-antigens. Several mechanisms safeguard immunological tolerance. These include removal of autoreactive T and B lymphoid cells by BIM-mediated apoptosis, both during their development in the thymus [3] or bone marrow [4] and as mature cells in the periphery [4], dampening the responsiveness of mature lymphocytes (anergy) [5] and control of effector T cells by regulatory T cells (T_{reg}). [5] Since apoptosis plays a critical role in lymphocyte selection and immune cell homeostasis, defects in its regulation have emerged as a cause of autoimmune disease. [5] FASL/FAS-mediated apoptosis signalling (known as the "death receptor" or "extrinsic" cell death pathway) imposes a critical barrier against autoimmune disease and lymphadenopathy. [6] Expression of the death receptor FAS (also called APO-1 or CD95) is virtually ubiquitous, presumably to allow FASL mediated killing of many cell types, when infected or stressed. [6] In contrast, FASL expression is restricted to activated T cells and NK cells, with its activity subject to post-translational control (e.g. proteolytic conversion of membrane-bound into secreted FASL). [6, 7]

Mice bearing spontaneously acquired or gene-targeting induced loss-of-function mutations in *Fas* (e.g. $Fas^{lpr/lpr}$, $Fas^{-/-}$), *FasL* (e.g. $FasL^{gld/gld}$, $FasL^{-/-}$) or those that lack membrane bound FASL ($FasL^{\Delta m/\Delta m}$) as well as humans with mutations in *Fas* (reviewed [6]) develop progressive lymphadenopathy and autoantibody-mediated pathology. The lymphadenopathy is characterised by large numbers of 'unusual' non-malignant, DN T cells ($TCR\alpha/\beta^{+}CD3^{+}CD4^{-}CD8^{-}B220^{+}$), which are thought to be previously activated $CD8^{+}$ T cells that have accumulated due to defective FASL/FAS-mediated apoptosis. [6] Experiments with $Fas^{lpr/lpr}$ mice expressing wild-type *Fas* transgenes in select cell types or

gene-targeted mice lacking FAS only in specific cell populations have shown that the lymphadenopathy results from the lack of FAS on T cells whereas loss of FAS on B cells causes autoantibody mediated SLE-like autoimmune pathology. [8]

The NF-κB transcription factor family regulates multiple aspects of the immune system including the control of cell survival, proliferation and differentiation. [9] Dysregulated activation of NF-κB effector pathways has been implicated in the pathogenesis of several autoimmune diseases. For example, abnormally increased numbers of cells with activated NF-κB have been found in tissues of mice or humans afflicted with SLE, rheumatoid arthritis or type 1 diabetes. [10] Blocking NF-κB activity may therefore constitute an attractive strategy for treating autoimmune and inflammatory disorders. However, current therapies that impact on NF-κB activity tend to inhibit all NF-κB proteins [11] and therefore frequently have undesired side effects, such as immune-suppression.

There are five members of the NF-κB family of transcription factors: RELA (p65), RELB, c-REL, NF-κB1 (p105/p50) and NF-κB2 (p100/p52). These proteins can form various hetero- and homo-dimers that can bind to specific sequences (κB sites) in the genome to regulate expression of target genes. [9] The activation of NF-κB transcription factors is subject to elaborate control, including proteolytic processing of precursor proteins and retention of complexes in the cytoplasm by IκB inhibitory proteins. [12] The signalling cascades responsible for the activation of the NF-κB transcription factors have been divided into the canonical and non-canonical pathways. These pathways are activated by distinct upstream signals, such as stimulation of cytokine receptors or B- and T- cell antigen receptors for the canonical pathway (involving mostly dimers containing c-REL or RELA and p50-NF-κB1) or stimulation of certain TNFR family members (e.g. BAFF-R, mostly to activate p52-NF-κB2/RELB heterodimers) for the non-canonical pathway. [9] Many NF-κB target genes encode cytokines, chemokines or other factors that control innate as well as adaptive immune responses. [9]

The critical role of the NF-κB signalling pathways in the immune system and the presence of abnormally increased numbers of leukocytes with activated NF-κB in tissues of SLE patients [13] prompted us to investigate the individual roles of c-REL, NF-κB1 and NF-κB2 in this disease using the *Fas*$^{lpr/lpr}$ mouse model. These NF-κB transcription factors were selected due to their prominent functions in the canonical or non-canonical NF-κB pathways, respectively, and because they are primarily required for immune cell function but not embryogenesis or haematopoietic cell differentiation. [9] While NF-κB1 is expressed ubiquitously and NF-κB2 is broadly expressed, the mainly haematopoietic cell restricted expression of c-REL [9] provides the advantage of primarily

targeting immune functions in mice deficient for this gene.

Mice lacking c-REL develop normally and appear healthy but exhibit defective activation of B and T lymphocytes, macrophages and dendritic cells (DCs) that collectively result in a deficit in antibody and cytokine production. [9] The *nfkb1*$^{-/-}$ mice develop normally and appear healthy until approximately one year of age but later develop a premature aging syndrome. [14] Young (healthy) *nfkb1*$^{-/-}$ mice exhibit defects in both adaptive and innate immune responses, particularly those involving B cells and macrophages. [15] The *nfkb2*$^{-/-}$ mice develop normally and initially appear healthy, but with increasing age they exhibit (relatively minor) multi-organ leukocyte infiltrates and mild autoimmune disease. [16] The *nfkb2*$^{-/-}$ mice also have impaired humoral immune responses due to a deficit in mature B cells, caused by defects in their survival and germinal center formation. [17]

Our studies reported here reveal that only the loss of c-REL significantly prolongs the lifespan and substantially diminishes glomerulonephritis (GN) in *Fas*$^{lpr/lpr}$ mutant mice, whereas loss of either NF-κB1 or NF-κB2 had only minor impact on the lifespan of these autoimmune disease-prone animals. This suggests that selective targeting of c-REL may represent a promising strategy for the treatment of certain autoimmune diseases.

RESULTS

Loss of c-REL greatly prolongs the lifespan of *Fas*$^{lpr/lpr}$ mice, whereas loss of NF-κB1 or NF-κB2 only has a modest impact

We inter-crossed *Fas*$^{lpr/lpr}$ mutant mice with mice lacking NF-κB1, NF-κB2 or c-REL (all parental strains on a C57BL/6 background). Mice deficient for both FAS and individual NF-κB family members (*Fas*$^{lpr/lpr}$*nfkb1*$^{-/-}$, *Fas*$^{lpr/lpr}$*nfkb2*$^{-/-}$ or *Fas*$^{lpr/lpr}$*c-rel*$^{-/-}$) were compared to control animals including, wt, *Fas*$^{lpr/lpr}$, *nfkb1*$^{-/-}$, *nfkb2*$^{-/-}$ and *c-rel*$^{-/-}$ mice over a two-year time frame.

Loss of NF-κB1 or NF-κB2 modestly (albeit significantly) extended the lifespan of *Fas*$^{lpr/lpr}$ mice (median survival: *Fas*$^{lpr/lpr}$*nfkb1*$^{-/-}$ 449 vs *Fas*$^{lpr/lpr}$ 402 days, p=0.0066; *Fas*$^{lpr/lpr}$*nfkb2*$^{-/-}$ 445 vs *Fas*$^{lpr/lpr}$ 402 days, p=0.0124; Figure 1a). Notably, *Fas*$^{lpr/lpr}$*nfkb1*$^{-/-}$ and *Fas*$^{lpr/lpr}$*nfkb2*$^{-/-}$ mice all had substantially shorter lifespans compared to their *nfkb1*$^{-/-}$ or *nfkb2*$^{-/-}$ parental controls (Figure 1a). Remarkably, loss of c-REL prolonged the lifespan of *Fas*$^{lpr/lpr}$ mice substantially (median survival: *Fas*$^{lpr/lpr}$*c-rel*$^{-/-}$ 685 vs *Fas*$^{lpr/lpr}$ 402 days, p<0.0001, Figure 1a). These results indicate that cellular processes dependent on c-REL are critical for the pathologies responsible for the early mortality of *Fas*$^{lpr/lpr}$ mice.

The major causes of morbidity and premature death of *Fas*$^{lpr/lpr}$ mice are lymphadenopathy and glomerulonephritis (GN), the latter elicited (at least in part) by immune complex deposition on the glomerular basement membrane (GBM), an increase in the number of cells in the glomerulus (mesangial cell proliferation) and leukocyte infiltration.[18] The incidence, severity and time of onset of GN and lymphadenopathy in *Fas*$^{lpr/lpr}$ mice are greatly affected by genetic background. Even though *Fas*$^{lpr/lpr}$ mice on the C57BL/6 background have relatively mild and late onset of autoimmune pathology [19] at ~410 days, IgM, IgG and IgA containing immune complex deposits were readily detectable in the renal glomerular capillary loops in our cohort (Figure 1b, arrows). In contrast, this pathology was only rarely seen in similarly aged or even older *Fas*$^{lpr/lpr}$ mice lacking NF-κB1, NF-κB2 or c-REL (Figure 1b and unpublished) and was absent in the parental *nfkb1*$^{-/-}$, *nfkb2*$^{-/-}$ and *c-rel*$^{-/-}$ mice (Supplementary Figure 1). In old *Fas*$^{lpr/lpr}$ mice lacking NF-κB1, NF-κB2 or c-REL the few detectable immune complex deposits were confined to mesangial cells and mostly consisted of IgM but not IgG or IgA (Figure 1b). Notably, immune complex deposition on mesangial cells and IgM containing immune complexes are not usually associated with glomerular destruction. [20] However, extensive glomerular damage, including glomerular hyper-cellularity with leukocyte infiltration (pathology grading 2-4) was observed in *Fas*$^{lpr/lpr}$*nfkb1*$^{-/-}$ and *Fas*$^{lpr/lpr}$*nfkb2*$^{-/-}$ mice with similar severity compared to *Fas*$^{lpr/lpr}$ controls (*Fas*$^{lpr/lpr}$*nfkb1*$^{-/-}$ vs *Fas*$^{lpr/lpr}$, p=ns, *Fas*$^{lpr/lpr}$*nfkb2*$^{-/-}$ vs *Fas*$^{lpr/lpr}$, p=ns, Figure 1c,d). Notably mice lacking NF-κB1 alone had a low incidence of GN themselves (Figure 1c), while mice lacking

either NF-κB2 or c-REL did not develop GN. [21] Loss of c-REL caused the most profound reduction in renal pathology (*Fas*$^{lpr/lpr}$*c-rel*$^{-/-}$ vs *Fas*$^{lpr/lpr}$, p=0.0019, Figure 1c,d), manifest as a marked reduction in glomerular hyper-cellularity and leukocyte infiltration, capillary loop obliteration and fibroid necrosis. These results show that loss of c-REL prolongs the lifespan of *Fas*$^{lpr/lpr}$ mutant mice by reducing both glomerular hyper-cellularity, leukocyte infiltration and immune complex deposit mediated pathology in the kidney (and possibly other tissues).

Impact of loss of NF-κB1, NF-κB2 or c-REL on cytokine and chemokine levels in *Fas*$^{lpr/lpr}$ mice

Prior to the onset of overt SLE-like autoimmune pathology, *Fas*$^{lpr/lpr}$ mice (on both an MRL and C57BL/6 background) have abnormally increased levels of many cytokines and chemokines in their sera. We measured the serum levels of 23 cytokines and chemokines and confirmed that the inflammatory cytokines IFNγ, IL-1β, IL-5, IL-6, IL-12, IL-17, plus the chemokines MIP1β, Eotaxin and MCP-1 were elevated at 5 months of age in *Fas*$^{lpr/lpr}$ mice compared to wt controls; this was particularly prominent for IFNγ, IL-17 and IL-12 (Figure 2). Since the NF-κB pathways control the expression of a broad range of cytokines and chemokines [9], we examined the impact of the absence of NF-κB1, NF-κB2 or c-REL on the levels of these immune regulators in *Fas*$^{lpr/lpr}$ mice. Loss of NF-κB1 reduced the levels of IL-5, a cytokine known to stimulate B cell maturation and Ig production (*Fas*$^{lpr/lpr}$ vs *Fas*$^{lpr/lpr}$*nfkb1*$^{-/-}$ $p<0.05$). However, IL-6 levels remained elevated in *Fas*$^{lpr/lpr}$*nfkb1*$^{-/-}$ and *Fas*$^{lpr/lpr}$*nfkb2*$^{-/-}$ mice (Figure 2), consistent with the inflammatory and autoimmune abnormalities observed in the aged parental *nfkb1*$^{-/-}$ and *nfkb2*$^{-/-}$ mice. [14, 16] In *Fas*$^{lpr/lpr}$*c-rel*$^{-/-}$ mice the levels of IL-5, IL-6, IL-12, IL-17, IFNγ, MIP-1β, MCP–1 and Eotaxin were all significantly reduced compared to those found in *Fas*$^{lpr/lpr}$ animals (Figure 2). These results reveal that c-REL and (to a lesser extent) NF-κB1 and NF-κB2 are critical for the abnormal increase in inflammatory cytokines and chemokines found in *Fas*$^{lpr/lpr}$ mice.

Impact of NF-κB family members acting in the canonical or non-canonical NF-κB pathways on the lymphadenopathy in *Fas*$^{lpr/lpr}$ mice

Progressive lymphadenopathy and splenomegaly are characteristic features of mice and humans deficient in FASL or FAS. [6] Abnormal accumulation of lymphocytes (largely composed of the so-called 'unusual' DN T cells) is thought to be due to their defect in "activation induced cell death" (AICD), a process mediated by FASL/FAS-induced apoptosis. [6]. Consistent with previous reports [22], our *Fas*$^{lpr/lpr}$ mice (on a C57BL/6 background) displayed early signs of lymphadenopathy and

splenomegaly with the associated accumulation of DN T cells from 12 weeks, and the severity of these abnormalities increased progressively thereafter with age (Figure 3a,b). Unexpectedly, loss of NF-κB2 substantially accelerated the onset and increased the magnitude of lymphadenopathy and splenomegaly in *Fas*$^{lpr/lpr}$ mice (Figure 3a). This was evident from 6 weeks of age (Figure 3a, spleen; *Fas*$^{lpr/lpr}$*nfkb2*$^{-/-}$ vs *Fas*$^{lpr/lpr}$ $p<0.005$) and was accompanied by an accelerated accumulation of DN T cells (Figure 3b, spleen; *Fas*$^{lpr/lpr}$*nfkb2*$^{-/-}$ vs *Fas*$^{lpr/lpr}$ $p<0.0005$, 20 weeks). By 12 weeks, DN T cells composed the majority of leukocytes within the peripheral lymph nodes and spleen of *Fas*$^{lpr/lpr}$*nfkb2*$^{-/-}$ mice (*Fas*$^{lpr/lpr}$*nfkb2*$^{-/-}$ vs *Fas*$^{lpr/lpr}$; lymph nodes $153.8x10^7 \pm 29.27x107$ $p=0.0251$, spleen $92.4x10^7 \pm 13.6x10^7$, $p=0.00498$, Figure 3b, Supplementary Figure 2). The *Fas*$^{lpr/lpr}$*nfkb2*$^{-/-}$ mice exhibited a 30-fold and 9-fold increase, respectively, in lymph node and splenic cellularity compared to *Fas*$^{lpr/lpr}$ mice, and a 73-fold and 10-fold increase in the lymph node and splenic cellularity, respectively, compared to wt mice (Figure 3c). In contrast, loss of NF-κB1 delayed the onset and diminished the extent of the accumulation of DN T cells in the spleen (12 weeks, $p=0.00610$, Figure 3b, Supplementary Figure 2) and lymph nodes (12 weeks, $p=0.0365$, Figure 3b, Supplementary Figure 2) of *Fas*$^{lpr/lpr}$ mice. Notably, by 20 weeks of age the total lymph node and splenic cellularity in *Fas*$^{lpr/lpr}$*nfkb1*$^{-/-}$ were similar to those seen in wt animals (Figure 3c). Loss of c-REL had no impact on the rate of onset or magnitude of lymphadenopathy and splenomegaly (Figure 3a,c) or the accumulation of DN T cells in *Fas*$^{lpr/lpr}$ mice (20 weeks of age: *Fas*$^{lpr/lpr}$*c-rel*$^{-/-}$ vs *Fas*$^{lpr/lpr}$ p=ns, Figure 3b and Supplementary Figure 2). These results show that NF-κB1 is critical for the development of lymphadenopathy, splenomegaly and accumulation of DN T cells in *Fas*$^{lpr/lpr}$ mice whereas NF-κB2 restrains this pathology and c-REL has no essential role. Furthermore, these data suggest that the lymphadenopathy is not a major driver of the mortality in *Fas*$^{lpr/lpr}$ mice.

Impact of loss of NF-κB1, NF-κB2 or c-REL on hyper-gammaglobulinaemia and autoantibody levels in *Fas*$^{lpr/lpr}$ mice

Mice and humans with SLE often display polyclonal hyper-gammaglobulinaemia as a consequence of excessive Th2 cell mediated activation and differentiation of B cells into antibody-secreting plasma cells. NF-κB1, NF-κB2 and c-REL all play critical roles in B cell activation, survival and Ig class switching and, accordingly, mice lacking these transcription factors have abnormally reduced serum IgG, IgA and IgE levels. [15, 23, 24] We examined the impact of loss of NF-κB1, NF-κB2 or c-REL on the hyper-gammaglobulinaemia in *Fas*$^{lpr/lpr}$ mice. At 5 months of age our *Fas*$^{lpr/lpr}$ mice (on a C57BL/6 background) had abnormally high levels of serum IgG1, IgG2a, IgG2b and IgA (Figure 3d). Loss of

NF-κB1, NF-κB2 or c-REL reduced the levels of IgG1 and IgA in *Fas*$^{lpr/lpr}$ mice compared to those seen in wt controls (Figure 3d).

High anti-nuclear autoantibody (ANA) levels are diagnostic for SLE (and certain other autoimmune diseases) in both humans and mice, including the *Fas*$^{lpr/lpr}$ strain. [6, 19] Consistent with previous reports [19], we found that sera from 20 week-old *Fas*$^{lpr/lpr}$ mice, but not those from wt animals, contained autoantibodies that produced a characteristic homogeneous nuclear staining in fixed HepG2 cells (Figure 3e,f; *Fas*$^{lpr/lpr}$ vs wt: $p<0.0005$). High levels of anti-nuclear autoantibodies in *Fas*$^{lpr/lpr}$ mice were also confirmed by ELISA (Figure 3f). Notably, the loss of NF-κB1, NF-κB2 or c-REL significantly reduced the levels of ANA in *Fas*$^{lpr/lpr}$ mice (*Fas*$^{lpr/lpr}$*nfkb1*$^{-/-}$ vs *Fas*$^{lpr/lpr}$ $p<0.0005$, *Fas*$^{lpr/lpr}$*nfkb2*$^{-/-}$ vs *Fas*$^{lpr/lpr}$ $p<0.001$, *Fas*$^{lpr/lpr}$*c-rel*$^{-/-}$ vs *Fas*$^{lpr/lpr}$ $p<0.05$ Figure 3e,f).

Next we assayed the levels of organ-specific autoantibodies by staining an array of tissues from *rag1*$^{-/-}$ mice (to remove endogenous Ig, a source of background staining) with sera from the different mouse strains. Aged *Fas*$^{lpr/lpr}$ mice had readily detectable autoantibodies (IgG, IgM and IgA) that stained lung epithelia, liver, the submandibular gland, thyroid follicles, gastric parietal cells and pancreatic acinar cells (Supplementary Figure 3, Table 1). Sera from *c-rel*$^{-/-}$ mice had even lower levels of autoantibodies than wt animals (Supplementary Figure 3, Table 1). Interestingly, some *nfkb1*$^{-/-}$ and *nfbk2*$^{-/-}$ mice did contain organ-specific autoantibodies, although the intensity of staining and the frequency of tissues stained were considerably lower compared to the staining produced by sera from *Fas*$^{lpr/lpr}$ mice (Supplementary Figure 3, Table 1). Loss of NF-κB1 or NF-κB2 diminished the levels of organ-specific autoantibodies in *Fas*$^{lpr/lpr}$ mice. The sera from *Fas*$^{lpr/lpr}$*c-rel*$^{-/-}$ mice had the largest reduction in organ-specific autoantibodies, with their levels comparable to those seen in wt animals (Supplementary Figure 3, Table 1). Collectively, these results demonstrate that while NF-κB1, NF-κB2 and c-REL all contribute to the development of hyper-gammaglobulinaemia and the production of ANA as well as organ-specific auto-antibodies in *Fas*$^{lpr/lpr}$ mice, loss of c-REL had the most pronounced impact on antibody mediated pathologies.

Impact of loss of NF-κB1, NF-κB2 or c-REL on lymphocyte infiltration into organs in *Fas*$^{lpr/lpr}$ mice

A comparison of the nature, severity and onset of autoimmune pathologies in control *Fas*$^{lpr/lpr}$ mice and *Fas*$^{lpr/lpr}$ mice lacking NF-κB1, NF-κB2 or c-REL was conducted at 5 months of age by undertaking a histological analysis of lung, liver and salivary gland (Figure 4a). While no lung pathology was evident

in the *Fas*$^{lpr/lpr}$ mice, severe peri-bronchial and peri-vascular lymphocyte infiltrations were observed in all *Fas*$^{lpr/lpr}$*nfkb2*$^{-/-}$ mice, consistent with interstitial lymphoid pneumonitis (*Fas*$^{lpr/lpr}$*nfkb2*$^{-/-}$ vs *Fas*$^{lpr/lpr}$, Figure 4a, summarised in Figure 4b, $p<0.0005$). Interestingly, minor lymphocytic infiltrations were observed in the lungs of *nfkb2*$^{-/-}$ mice (Figure 4a,b), consistent with the report that these animals develop mild autoimmune disease. [17] Discrete peri-vascular inflammatory lesions were also evident in the livers of *FasL*$^{lpr/lpr}$*nfkb2*$^{-/-}$ animals, but this was rarely observed in the livers of age-matched wt, *Fas*$^{lpr/lpr}$, *nfkb1*$^{-/-}$, *Fas*$^{lpr/lpr}$*nfkb1*$^{-/-}$, *c-rel*$^{-/-}$ or *Fas*$^{lpr/lpr}$*c-rel*$^{-/-}$ mice (Figure 4a,b). The lymphoid accumulations in the lungs of *Fas*$^{lpr/lpr}$*nfkb2*$^{-/-}$ mice were mainly composed of DN T cells and the polyclonal nature of this lymphoid infiltrate revealed through diverse TCR Vβ usage, demonstrated that these infiltrating T cells were not part of a malignant lymphoma (Supplementary Figure 4). These observations show that loss of NF-κB2 exacerbates lymphocyte infiltration into the lungs and other tissues in *Fas*$^{lpr/lpr}$ mice.

Impact of loss of NF-κB1, NF-κB2 or c-REL on autoimmune dermatitis in *Fas*$^{lpr/lpr}$ mice

Upon injection with dendritic cells that had been exposed to necrotic cell debris, *Fas*$^{lpr/lpr}$ mice on the MRL background were found to develop a 'butterfly'-shaped facial lesion [25], reminiscent of the malar rash (atopic dermatitis) observed in human SLE patients. Although *Fas*$^{lpr/lpr}$ mice on a C57BL/6 background do not spontaneously develop this pathology (unpublished results), we found that a number of ageing *Fas*$^{lpr/lpr}$*c-rel*$^{-/-}$ mice presented with hair loss across the bridge of the nose and eye lids accompanied by thickening and scabbing of the skin (Figure 4c). Autoimmune dermatitis in both humans [26] and mice [7] is frequently associated with abnormally elevated serum IgE levels. However, we did not observe this association in the mouse models described here. Only *Fas*$^{lpr/lpr}$ mice, which do not exhibit the dermatitis, had elevated serum IgE levels (Figure 4d).

Reduced numbers and/or function of Foxp3$^+$ regulatory T cells (T_{regs}), a CD4$^+$ T-cell population essential for preventing fatal, multi-organ autoimmune disease, has been implicated in hyper-IgE and autoimmune dermatitis. [27] Therefore, we measured the numbers of CD4$^+$CD25$^+$Fox3p$^+$ T_{reg} cells in parental *Fas*$^{lpr/lpr}$ mice and *Fas*$^{lpr/lpr}$ mice lacking NF-κB1, NF-κB2 or c-REL by flow cytometric analysis. Loss of NF-κB1 resulted in a mild reduction in T_{reg} cells (6 and 12 weeks, Figure 5b), while loss of NF-κB2 (both in the absence or presence of the *Fas*$^{lpr/lpr}$ mutation) had little effect on the percentages of T_{reg} cells in the peripheral lymphoid organs. However due to the development of splenomegaly (Figure 3c), particularly in the *Fas*$^{lpr/lpr}$*nfkb2*$^{-/-}$ mice, an elevation in the total numbers of splenic T_{reg} cells was observed (Figure 5b). c-REL was shown to be essential for the development of

$CD4^+CD25^+FOXP3^+$ T_{reg} cells [28] and, accordingly, we found that loss of c-REL significantly reduced T_{reg} cell numbers in the peripheral lymphoid organs of *Fas*$^{lpr/lpr}$ mice (for example, spleen at 6 weeks; *Fas*$^{lpr/lpr}$ vs *Fas*$^{lpr/lpr}$*c-rel*$^{-/-}$ $p<0.0005$, Figure 5a and total T_{regs} spleen; *Fas*$^{lpr/lpr}$*c-rel*$^{-/-}$ vs *c-rel*$^{-/-}$ $p<0.05$, Figure 5b). These results indicate that while a defect in T_{reg} cells may not be critical for the development of many of the autoimmune pathologies (e.g. GN) observed in the *Fas*$^{lpr/lpr}$ mice, the reduction in T_{reg} cells, caused by loss of c-REL, may cooperate with loss of FASL/FAS-mediated apoptosis signalling to elicit autoimmune dermatitis.

Defects in thymic tolerance may contribute to the exacerbated leukocyte infiltration into organs observed in *Fas*$^{lpr/lpr}$*nfkb2*$^{-/-}$ mice

Thymic epithelial cells play critical roles in central tolerance to tissue-specific antigens. [29] Deficiencies in the number or function of medullary thymic epithelial cells (mTECs) have been associated with organ-specific autoimmune disease mediated by auto-reactive T cells that have escaped negative selection. [29, 30] Loss of FASL or FAS causes abnormal survival of auto-reactive or chronically stimulated mature T and B cells in peripheral lymphoid organs but has no impact on the deletion of auto-reactive T and B lymphoid cells in the thymus or bone marrow, respectively. [6] The canonical NF-κB pathway plays essential roles in the stepwise differentiation and selection of T cells. [31] Conversely, the non-canonical NF-κB pathway is critical for the development, survival and function of thymic epithelial cells (TECs). [29, 32] NF-κB2 deficiency was reported to cause a reduction in $CD80^+$ mTECs but had no impact on the numbers of mTECs that express the autoimmune regulator AIRE. [16] We conducted a detailed analysis of the thymic microenvironment to examine whether mTEC defects might be responsible for the autoimmune and lympho-proliferative pathologies observed in *Fas*$^{lpr/lpr}$ mice and/or the impact of loss of NF-κB1, NF-κB2 or c-REL on the *Fas*$^{lpr/lpr}$ disease profile.

Thymic sections from 6 or 20-week-old mice were stained with a variety of markers (keratin-5 (K5), UEA-1 and AIRE) to define the major mTEC subsets and the medullary architecture. The medullary composition and distribution of $AIRE^+$ mTEC in *Fas*$^{lpr/lpr}$ were comparable to those of age-matched wt mice (Figure 6a,b). The expression patterns of mTEC markers in the thymi of *nfkb1*$^{-/-}$, *c-rel*$^{-/-}$, *Fas*$^{lpr/lpr}$*nfkb1*$^{-/-}$ and *Fas*$^{lpr/lpr}$*c-rel*$^{-/-}$ mice were also comparable to those seen in wt controls (Figure 6a,b). In contrast, thymi from *nfkb2*$^{-/-}$ and *Fas*$^{lpr/lpr}$*nfkb2*$^{-/-}$ mice had reduced numbers of UEA-1 expressing cells, smaller medullary islets due to the loss of mTECs, defined by $K5^+$ cells, and reduced numbers of $AIRE^+$ mTECs (from 20 weeks, Figure 6a,b). Flow cytometric analysis of thymic stromal cells was performed to determine the number and phenotype of cortical TEC (cTEC) and mTEC

subsets expressing high or low levels of MHC class II (mTEC^{hi} or mTEC^{lo}, respectively) among the various mouse strains (Figure 6c). The numbers of mTEC^{hi} cells were substantially diminished in thymi from *nfkb1*$^{-/-}$, but not *Fas*$^{lpr/lpr}$*nfkb1*$^{-/-}$, mice and to an even greater extent in *nfkb2*$^{-/-}$ and *Fas*$^{lpr/lpr}$*nfkb2*$^{-/-}$ mice (Figure 6c). Remarkably, AIRE^{+} TECs were almost completely absent in the *nfkb2*$^{-/-}$ and *Fas*$^{lpr/lpr}$*nfkb2*$^{-/-}$ mice (*Fas*$^{lpr/lpr}$*nfkb2*$^{-/-}$ were ~10% of wt numbers; Figure 6d). These results demonstrate that *Fas*$^{lpr/lpr}$ mice have a normal TEC composition, indicating that FAS has no major role in TEC development and survival. Since the loss of AIRE expressing mTECs can impair negative selection of auto-reactive thymocytes and thereby lead to autoimmune disease [29], the mild autoimmunity in *nfkb2*$^{-/-}$ mice [16] and the exacerbated organ-specific lymphocyte infiltration observed in *Fas*$^{lpr/lpr}$*nfkb2*$^{-/-}$ animals may be explained (at least in part) by the deficit in mTECs in these animals.

DISCUSSION

Although autoimmune diseases are relatively prevalent, much remains to be learnt about the defects in signalling pathways that are responsible for their development and progression. The canonical and non-canonical NF-κB signal transduction pathways regulate a broad range of genes and biological processes that control pathogen directed immune responses, but when dysregulated, they can promote autoimmunity. It is therefore possible that members of the NF-κB protein family play a role in the pathogenesis of autoimmune diseases and may thus represent attractive therapeutic targets. Notably, the immunosuppressive and anti-inflammatory activities of NSAIDs (non-steroidal anti-inflammatory drugs) and glucocorticoids, widely used for the treatment of several autoimmune diseases, are (at least partly) due to their ability to dampen NF-κB activation. [33] However, since NF-κB activation regulates a wide variety of processes, both within and outside the immune system, prolonged systemic blockade of NF-κB activity can have deleterious side effects, such as immune-suppression. [34] In this study we examined the roles of NF-κB1, NF-κB2 and c-REL in the autoimmune pathologies that arise in *Fas*$^{lpr/lpr}$ mice to gain insight into the potential utility of individually targeting these NF-κB family members as a therapeutic strategy for patients with autoimmune disease.

The *Fas*$^{lpr/lpr}$ mouse strain is a model of spontaneous SLE that exhibits many of the classical hallmarks of this complex autoimmune disease in humans, including autoantibody production and GN mediated in part by immune complex deposits in renal glomeruli. To date, the role of NF-κB signalling in the development of autoimmune disease in *Fas*$^{lpr/lpr}$ mice has not been explored in detail. Broad-spectrum pharmacological blockade of NF-κB activity was reported to reduce the severity of certain autoimmune manifestations in the SLE-predisposed FcγRIIb-deficient mice [35], but the impact on GN was not rigorously examined. Moreover, transgenic expression of a non-degradable form of IκBα (IκBSR) (a repressor of NF-κB activation) in T lymphocytes diminished, but did not prevent, autoimmune pathology in *FasL*$^{gld/gld}$ mutant mice. [36] The observation that the impact on autoimmune pathology in this model was rather modest may be attributed to the fact that NF-κB activity was only partially inhibited, and then, only in T lymphocytes. This latter point is pertinent, because experiments with mice with conditional ablation of the *Fas* gene demonstrated that the loss of FAS induced apoptosis of B cells is necessary for SLE-like autoimmune disease to occur. [8] Thus, the impact of loss of an individual NF-κB protein on autoimmune disease elicited by defects in FAS remains to be determined. Here we present the first comprehensive analysis of the impact of loss of NF-κB1 or c-REL (major

components of the canonical NF-κB pathway) or loss of NF-κB2 (major component of the non-canonical NF-κB pathway) on the multi-faceted autoimmune pathology in *Fas*$^{lpr/lpr}$ mice (Table 2).

Loss of NF-κB2 and hence, impaired non-canonical NF-κB signalling, had varied impact on the different pathologies of *Fas*$^{lpr/lpr}$ mice. Severe GN was unaffected but the lympho-proliferative disease was substantially accelerated and augmented. Therefore, we conclude that NF-κB2-dependent processes curtail the proliferative expansion and/or survival of the lymphoid cells that accumulate due to defects in FASL/FAS-mediated apoptosis. Several mechanisms may account for the enhanced lympho-proliferative disease in *Fas*$^{lpr/lpr}$*nfkb2*$^{-/-}$ mice. For instance, absence of the full-length NF-κB2 precursor protein, p100, which has IκB-like NF-κB repressor activity, may result in enhanced RELA-driven T cell proliferation. [37] Moreover, escape of thymocytes with autoreactive TCRs from negative selection as a consequence of the reduced numbers of AIRE expressing mTECS (due to loss of NF-κB2) may also contribute to enhanced T cell accumulation in *Fas*$^{lpr/lpr}$*nfkb2*$^{-/-}$ mice. The reduction in some aspects of autoantibody mediated pathology in *Fas*$^{lpr/lpr}$*nfkb2*$^{-/-}$ mice may be explained by reduced BAFF-R triggered survival signalling in B cells and/or defects in germinal center formation. These processes both involve p52-NF-κB2/RELB heterodimers. [38] It is, however, noteworthy that the canonical and non-canonical NF-κB signalling pathways were both reported to be critical for the SLE-like autoimmune disease elicited by transgenic overproduction of BAFF. [13] Our recent studies in *FasL* mutant mice revealed that loss of NF-κB2 reduced the levels of inflammatory cytokines, autoantibodies and even GN. [21] However, the impact on animal survival was minor, as similar to the present study, the exacerbated lymphadenopathy due to loss of FASL/FAS-mediated apoptosis caused severe lung pathology. [21] Even in humans, inactivating mutations in NF-κB2 have been associated with certain diseases, such as common variable immunodeficiency (CVID) [39] with autoimmune features, including hypo-gammaglobulinaemia, alopecia and recurrent infections, severe B cell deficiency and alopecia [40] or humoral immune deficiency also affecting T cell proliferation. [41] Hence, although systemic targeting of NF-κB2 would be expected to diminish autoantibody-induced pathology, the therapeutic benefit for SLE-like disease would likely be mitigated by exacerbated lympho-proliferative disease, as we have shown here, and significant immunodeficiency as indicated by the studies of human.

Loss of NF-κB1 resulted in a modest, albeit significant, prolongation of lifespan in *Fas*$^{lpr/lpr}$ mice. This was most likely due to reduced autoantibody-mediated pathology. Notably, lymphadenopathy was also substantially reduced and delayed in *Fas*$^{lpr/lpr}$*nfkb1*$^{-/-}$ mice compared to *Fas*$^{lpr/lpr}$ controls. This indicates that the proliferation and/or survival of DN T cells (or their immediate precursors) depend on this NF-κB protein. Experiments in which *Fas* was conditionally deleted in select cell types showed that the

lympho-proliferative component of the disease caused by defects in FASL/FAS-mediated apoptosis has little impact on the lifespan of mice. [42] Thus, the slight increase in the lifespan of *Fas*$^{lpr/lpr}$ mice afforded by loss of NF-κB1 is unlikely to be due to its ability to diminish lymphadenopathy in these animals but must instead be due a reduction in autoantibody mediated pathology. However, although loss of NF-κB1 reduced the levels of autoantibodies in *Fas*$^{lpr/lpr}$ mice, this benefit was likely offset by an increase in inflammatory signaling caused by the loss of the transcriptional repression activity of NF-κB1. It has been reported that NF-κB1 homodimers can recruit HDAC1 to κB sites in pro-inflammatory genes and thereby block their transcriptional induction by other NF-κB factors. [43] The resulting loss of transcriptional suppressive activity likely contributes to the ongoing inflammation observed in many organs of *Fas*$^{lpr/lpr}$*nfkb1*$^{-/-}$ mice (unpublished observations). This notion is consistent with a recent study showing that the reduced lifespan of *nfkb1*$^{-/-}$ mice could be attributed to chronic, progressive low-grade inflammation and premature aging. [14] Interestingly, in humans (certain Asian populations) the *NF-κB1*-94ins/del promoter polymorphism, resulting in reduced NF-κB1 protein expression is associated with increased cancer risk. [44] Thus, constitutive drug-mediated inhibition of NF-κB1 may exacerbate certain autoimmune pathologies by increasing inflammation and may also increase the risk of malignancy.

Loss of c-REL caused the largest extension of lifespan of *Fas*$^{lpr/lpr}$ mice, and this appeared to be due to the prevention of GN and autoantibody mediated pathologies. Interestingly, lymphadenopathy was unaffected by loss of c-REL. This finding was surprising considering that c-REL is critical for mitogen- or antigen-induced activation and proliferation of normal $CD4^+$ as well as $CD8^+$ T cells. [9, 24, 45] Coupled with our observation that lymphadenopathy was reduced in *Fas*$^{lpr/lpr}$*nfkb1*$^{-/-}$ mice compared to *Fas*$^{lpr/lpr}$ controls, we conclude that the proliferation of DN T cells (or their precursors) must be driven by hetero-dimers of p50-NF-κB1 and NF-κB family members other than c-REL (possibly RELA). Similar to our findings, loss of c-REL was shown to reduce or even prevent pathology in several mouse models of tissue-restricted autoimmune diseases, including collagen-induced arthritis, streptozotocin induced diabetes [9] and autoimmune encephalomyelitis (EAE) [46]. Indeed our own studies in a *FasL* mutant mouse model of SLE-like disease [21] also showed that loss of c-REL substantially extended animal lifespan, reduced many pathologies seen in this model, including GN, and reduced the levels of cytokines, chemokines as well as autoantibodies. [21]

c-REL is critical for Ig isotype switching, the differentiation and function of Th1 and Th17 [46] effector T cells, as well as the production of cytokines by macrophages and dendritic cells. [9] Although loss of c-

REL caused a reduction in T_{reg} cells [28], which was also observed in *Fas*$^{lpr/lpr}$*c-rel*$^{-/-}$ mice, this deficiency did not worsen autoimmune pathology in this model. Defects in the activation of conventional T and B cells caused by the loss of c-REL might explain this observation. [47] Surprisingly, our study revealed that loss of c-REL resulted in the spontaneous development of autoimmune facial dermatitis in *Fas*$^{lpr/lpr}$ mice, demonstrating that c-REL has a role in preventing this pathology in mice that lack FAS. Abnormally high serum IgE levels are associated with autoimmune dermatitis in both human patients and murine models. [48, 49] However, serum IgE levels were not abnormally elevated in healthy or dermatitis afflicted *Fas*$^{lpr/lpr}$*c-rel*$^{-/-}$ mice, most likely due to the reported role for c-REL in Ig isotype switching to IgE. [50] Defects in T_{reg} cells have also been implicated in autoimmune dermatitis. For example, mutations in Foxp3, the master regulator of T_{reg} cell development and function, cause eczema in both humans and mice. [51] We propose that the loss of FAS-induced apoptosis of auto-reactive B and T lymphocytes in the periphery and a reduction in T_{reg} cell exerted control of effector T cells (due to loss of c-REL) cooperate to elicit the autoimmune skin disease observed in *Fas*$^{lpr/lpr}$*c-rel*$^{-/-}$ mice.

Interestingly, polymorphisms in the *c-REL* gene have been linked to increased susceptibility to certain human autoimmune diseases, such as arthritis psoriasis, and celiac disease. [47] These observations and our discovery that constitutive loss of c-REL substantially prolongs the lifespan of *Fas*$^{lpr/lpr}$ mice by preventing autoantibody-mediated pathology identify c-REL (as well as its regulators and effectors) as suitable therapeutic targets. The notion that c-REL blockade is an effective suppressor of immune pathology is supported by a recent report describing that a small molecule inhibitor of c-REL could reduce allo-antigen induced T cell activation in allogenic bone marrow stem cell transplantation. [52]

METHODS

Mice

All experiments with mice were approved by the Animal Ethics Committee of the Walter and Eliza Hall Institute of Medical Research. *Fas*$^{lpr/lpr}$ mutant mice on a C57BL/6 background have been described. [19] The *nfkb1*$^{-/-}$ [15], *nfkb2*$^{-/-}$ [23] and *c-rel*$^{-/-}$ [24] mice were originally generated on a mixed C57BL/6x129SV background using 129SV derived ES cells and were subsequently backcrossed in our laboratory for >10 generations onto a C57BL/6 background. *Fas*$^{lpr/lpr}$ mice were intercrossed with *nfkb1*$^{-/-}$, *nfkb2*$^{-/-}$ or *c-rel*$^{-/-}$ mice and the resultant *Fas*$^{wt/lpr}$*nfkb1*$^{+/-}$, *Fas*$^{wt/lpr}$*nfkb2*$^{+/-}$ or *Fas*$^{wt/lpr}$*c-rel*$^{+/-}$ offspring were intercrossed to produce *Fas*$^{lpr/lpr}$*nfkb1*$^{-/-}$, *Fas*$^{lpr/lpr}$*nfkb2*$^{-/-}$ or *Fas*$^{lpr/lpr}$*c-rel*$^{-/-}$ mice. C57BL/6 (wt), *Fas*$^{lpr/lpr}$, *nfkb1*$^{-/-}$, *nfkb2*$^{-/-}$ and *c-rel*$^{-/-}$ mice were maintained in the same colony and were used as controls.

Histological Preparation and Scoring

Mice were killed by CO_2 asphyxiation and lung, liver, pancreas, salivary gland, lacrimal gland, and stomach were resected and fixed for microscopic analysis in 80% Histochoice (Amresco, Solon, OH, USA)/20% methanol and paraffin embedded. Conventional histopathology was performed on haematoxylin plus eosin (H&E) stained tissue sections. Lymphocytic infiltrates into the lung, liver, kidney, pancreas and sub-mandibular gland were assessed on H&E stained sections and graded 0-3, 0 = none, 1 = occasional small peri-vascular foci (age related), 2 = more dense well-defined peri-vascular and peri-ductal foci, 3 = extensive infiltrate with parenchymal destruction. H&E stained sections of kidneys were examined in a double blinded manner by a clinical nephrologist (PH) for evidence of glomerulonephritis and scored on a scale of 0-4 (0 = normal, 1 = minor mesangial hyper-cellularity, 2 = moderate glomerular hyper-cellularity, 3 = severe glomerular hyper-cellularity with thickening of capillary loops, 4 = severe glomerular hyper-cellularity with thickening and obliteration of all capillary loops and marked distortion of the glomerular tuft or fibrinoid necrosis or crescent formation). All photo-micrographs were obtained using a 10x/NA 0.3 objective lens on an Axioplan 2 microscope (Carl Zeiss MicroImaging, Inc, North Ryde, NSW, Australia.)

Flow Cytometric Analysis

Single cell suspensions of lymph nodes (pooled axillary, brachial, inguinal, mesenteric) and spleen of 6, 12 or 20-week old mice were stained as previously described [7] with FITC-, R-PE- or APC-conjugated surface marker specific mAbs (RB6-8C5: anti-Gr-1, MI/70: anti-Mac-1, M3/84.6.34: anti-

Mac-2, Ter119: anti-erythroid cell surface marker, F4/80: anti-macrophage surface marker, T24.31.2: anti-Thy-1, GK1.5: anti-CD4, 53.6.72: anti-CD8, RA3-6B2: anti-CD45R-B220, PK136: anti-NK1.1 (BD Biosciences, Franklin Lakes, NJ, USA) plus the vital dye PI (1 μg/mL). $CD4^+CD25^+Foxp3^+$ T_{reg} cells were detected after fixation and permeabilisation (eBiosciences, San Diego, USA) by staining with the following fluorochrome-conjugated monoclonal antibodies: FITC anti-CD4, R-PE anti-CD25 (Biolegend, San Diego, CA, USA) and APC anti-Foxp3 (eBiosciences).

Single cell suspensions were prepared from lungs by digestion for 20 min at room temperature with collagenase/DNase (7 mg collagenase (Worthington, Lakewood, NJ, USA) in 1 mL of 0.1% w/v DNase1 (Roche, Mannheim, Germany)) followed by treatment with ethylene-diaminetetra-acetic acid (EDTA) as described [21], followed by staining with an R-PE coupled antibody to Thy-1 plus a panel of biotinylated antibodies specific for different TCRVβ chains. This was followed by staining with FITC-coupled streptavidin (BD-Pharmingen). Flow cytometric analysis was performed on a FACScan or LSRII (Becton Dickson).

Serum Immunoglobulin Levels

Serum immunoglobulin levels were determined by ELISA as described [7]. Briefly, sheep anti-mouse Ig antibodies (Silenus Laboratories, Australia) were used as a capture reagent and bound antibodies from sera were revealed with mouse Ig isotype-specific goat antibodies that had been conjugated to horseradish peroxidase (Southern Biotechnology, AL, USA). Purified myeloma proteins were used as standards (Sigma, MO, USA).

Immunofluorescent Staining and Confocal Microscopy

Anti-nuclear auto-antibodies (ANA) in sera of aged or sick mice were detected by staining (1/100 serum dilution) slides coated with HEp-2 human epithelial cells (Immuno Concepts, Sacramento, CA, USA). Staining was visualised with FITC-conjugated goat antibodies against mouse IgG, IgA, IgM (Cappel, MP Biochemicals). ANA levels were semi-quantified in a blinded manner on a Leica laser scanning (SP2) confocal microscope according to brightness of fluorescence intensity, on a scale of 0 (no fluorescence) to 3+ (maximum fluorescence intensity). The levels of ANA in the sera of aged or sick mice were also quantified by ELISA (The Binding Site, Birmingham, UK) according to the manufacturer's instructions.

Auto-antibodies against antigens in tissues that are known targets of autoimmune attack in SLE and other autoimmune diseases (e.g. salivary gland, lacrimal gland, eye, kidney, liver, lung, pancreas, stomach, thyroid) were detected by staining of frozen tissue sections (5 μm, air dried and fixed in acetone) from *rag-1*$^{-/-}$ mice (to eliminate endogenous Ig as a source of background staining) with sera (1/100 dilution) from aged or sick mice. Staining was detected by using FITC-conjugated goat antibodies against mouse IgG, IgA and IgM (Cappel, MP Biochemicals).

To stain for immune complex deposits, kidneys from aged or sick mice were snap-frozen in isopentane, sectioned, acetone fixed, blocked with PBS/2% FCS and stained with FITC-coupled goat antibodies specific to mouse IgM, IgG or IgA (Southern Biotechnology, Birmingham, AL, USA) using counterstaining with DAPI to label nuclei. All immunofluorescent stained sections were analysed using a Leica SP2 confocal microscope.

Measurements of Serum Cytokine and Chemokine Levels

Serum cytokine and chemokine levels were measured using the Bio-Plex Pro™ mouse cytokine 23-plex (Bio-Rad, Gladesville, NSW, Australia) immunoassay kit following the manufacturers' instructions. The cytokines measured included: IL-1α, IL-β, IL-2, IL-3, IL-4, IL-5, IL-6, IL-9, IL-10, IL-12(p40), IL-12(p70), IL-13, IL-17A, eotaxin, G-CSF, GM-CSF, IFN-γ, KC (CXCL1), MCP-1, MIP-1α, MIP-1β, RANTES and TNFα.

Flow Cytometric Analysis of Thymic Stromal Cell Populations

This procedure has been described previously. [21] Connective tissue was removed from individual thymi (5 months), the lobes separated and the capsule cut with fine scissors. Thymi were then individually agitated in 10 mL RPMI-1640 medium for several minutes to gently flush out thymocytes using a wide-bore pipette. The thymic tissue remaining was then digested at 37°C with Liberase TM (0.5 Wunsch units (U) per mL, Roche) and DNase I (0.1% w/v), Sigma-Aldrich (St Louis, MO, USA) in RPMI-1640 medium with gentle agitation for 15 min. This process was repeated with the combined thymic fragments centrifuged, resuspended in PBS with 5 mM EDTA, 2% FCS and 0.02% NaN_3, filtered through a 100 μm mesh and counted. For phenotypic analysis 1.5 x 10^7 cells were stained with FITC-, R-PE-, PerCP/Cy5.5-, biotin or APC-conjugated surface marker specific mAbs (30-F11: anti-CD45 (Biolegend, San Diego, CA, USA), M5/114.15.2: anti-H2-AE (in house), G8.8: anti-EpCAM (in house), 6C3: anti-Ly51 (Biolegend), UEA-1 lectin (Vector Laboratories, Burlingame, CA, USA)). Biotinylated mAbs were detected with Streptavidin-PEcy7 (BD Biosciences). AIRE positive cells were detected after fixation by staining with APC-conjugated anti-AIRE antibodies (clone 5H12, in house). Flow cytometric analysis was performed on a LSRII (Becton Dickson).

Statistical Analysis

Statistical analysis was performed using the student's T-test, Mann Whitney U test or one-way ANOVA as indicated or log rank (Mantel-Cox) test for animal survival curves.

ACKNOWLEDGMENTS

We thank G Siciliano and K Hughes for animal care; J Corbin for automated blood analysis; B Helbert, C Young and Karen Mackwell for genotyping; E Tsui, V Babo, K Weston and all histology staff for preparation of histological sections. This work was supported by fellowships and grants from the NHMRC; Canberra; program #1016701, fellowships; (DG) #637353, #1090236 (DG), (AS) #1020363 and project grants; #1046010 (AS), #1009145 (LOR), #1049724 (DG), Australian Postgraduate Award (JL) and an NHMRC infrastructure grant, Independent Research Institutes Infrastructure Support Scheme Grant #361646, the Victorian State Government (OIS grant), the Leukemia and Lymphoma Society (SCOR grant #7413 and #7001-13) and the JDRF/NHMRC #466658 (AS). This research was also supported in part by the Intramural Research Program of the National Institute of Allergy and Infectious Diseases, National Institutes of Health (US).

Supplementary information is available at the Immunology & Cell Biology's website.

REFERENCES

1. Mok CC, Kwok RC, Yip PS. Effect of renal disease on the standardized mortality ratio and life expectancy of patients with systemic lupus erythematosus. *Arthritis Rheum* 2013; **65(8)**:2154-60.
2. Monneaux F, Muller S. Molecular therapies for systemic lupus erythematosus: clinical trials and future prospects. *Arthritis Res Ther* 2009; **11**(3):234.
3. Bouillet P, Purton JF, Godfrey DI, Zhang L-C, Coultas L, Puthalakath H, et al. BH3-only Bcl-2 family member Bim is required for apoptosis of autoreactive thymocytes. *Nature* 2002; **415**:922-6.
4. Enders A, Bouillet P, Puthalakath H, Xu Y, Tarlinton DM, Strasser A. Loss of the pro-apoptotic BH3-only Bcl-2 family member Bim inhibits BCR stimulation-induced apoptosis and deletion of autoreative B cells. *J Exp Med* 2003; **198**(7):1119-26.
5. Goodnow CC, Sprent J, Fazekas de St Groth B, Vinuesa CG. Cellular and genetic mechanisms of self tolerance and autoimmunity. *Nature* 2005; **435**(7042):590-7.
6. Strasser A, Jost PJ, Nagata S. The many roles of FAS receptor signaling in the immune system. *Immunity* 2009; **30(2)**:180-92.
7. O'Reilly LA, Tai L, Lee L, Kruse EA, Grabow S, Fairlie WD, et al. Membrane-bound Fas ligand only is essential for Fas-induced apoptosis. *Nature* 2009; **461(7264)**:659-63.
8. Hao Z, Duncan GS, Seagal J, Su YW, Hong C, Haight J, et al. Fas receptor expression in germinal-center B cells is essential for T and B lymphocyte homeostasis. *Immunity* 2008; **29(4)**:615-27.
9. Gerondakis S, Grumont R, Gugasyan R, Wong L, Isomura I, Ho W, et al. Unravelling the complexities of the NF-kappaB signalling pathway using mouse knockout and transgenic models. *Oncogene* 2006; **25(51)**:6781-99.
10. Pai S, Thomas R. Immune deficiency or hyperactivity-Nf-kappab illuminates autoimmunity. *J Autoimmun* 2008; **31(3)**:245-51.

11. Tak PP, Firestein GS. NF-kappaB: a key role in inflammatory diseases. *J Clin Invest* 2001; **107(1)**:7-11.

12. Hayden MS, Ghosh S. Shared principles in NF-kappaB signaling. *Cell* 2008; **132(3)**:344-62.

13. Enzler T, Bonizzi G, Silverman GJ, Otero DC, Widhopf GF, Anzelon-Mills A, et al. Alternative and classical NF-kappa B signaling retain autoreactive B cells in the splenic marginal zone and result in lupus-like disease. *Immunity* 2006; **25(3)**:403-15.

14. Jurk D, Wilson C, Passos JF, Oakley F, Correia-Melo C, Greaves L, et al. Chronic inflammation induces telomere dysfunction and accelerates ageing in mice. *Nature communications* 2014; **2**:4172.

15. Sha WC, Liou HC, Tuomanen EI, Baltimore D. Targeted disruption of the p50 subunit of NF-kappa B leads to multifocal defects in immune responses. *Cell* 1995; **80(2)**:321-30.

16. Zhang B, Wang Z, Ding J, Peterson P, Gunning WT, Ding HF. NF-kappaB2 is required for the control of autoimmunity by regulating the development of medullary thymic epithelial cells. *J Biol Chem* 2006; **281(50)**:38617-24.

17. Caamaño JH, Rizzo CA, Durham SK, Barton DS, Raventós-Suárez C, Snapper CM, et al. Nuclear Factor (NF)-κB2 (p100/p52) is required for normal splenic microarchitecture and B cell-mediated immune responses. *J Exp Med* 1998; **187(2)**:185-96.

18. Cohen PL, Eisenberg RA. *Lpr* and *gld*: single gene models of systemic autoimmunity and lymphoproliferative disease. *Annu Rev Immunol* 1991; **9**:243-69.

19. Izui S, Kelley VE, Masuda K, Yoshida H, Roths JB, Murphy ED. Induction of various autoantibodies by mutant gene lpr in several strains of mice. *J Immunol* 1984; **133(1)**:227-33.

20. Weening JJ, D'Agati VD, Schwartz MM, Seshan SV, Alpers CE, Appel GB, et al. The classification of glomerulonephritis in systemic lupus erythematosus revisited. *J Am Soc Nephrol* 2004; **15(2)**:241-50.

21. O'Reilly LA, Hughes P, Lin A, Waring P, Siebenlist U, Jain R, et al. Loss of c-REL but not NF-kappaB2 prevents autoimmune disease driven by FasL mutation. *Cell Death Differ* 2015; **22(5)**:767-78.

22. Hughes PD, Belz GT, Fortner K, Budd RC, Strasser A, Bouillet P. Apoptosis regulators Fas and Bim cooperate in shutdown of chronic immune responses and prevention of autoimmunity. *Immunity* 2008; **28(2)**:197-205.

23. Franzoso G, Carlson L, Poljak L, Shores EW, Epstein S, Leonardi A, et al. Mice deficient in nuclear factor (NF)-κB/p52 present with defects in humoral responses, germinal center reactions, and splenic microarchitecture. *J Exp Med* 1998; **187(2)**:147-59.

24. Köntgen F, Grumont RJ, Strasser A, Metcalf D, Li R, Tarlinton D, et al. Mice lacking the c-*rel* proto-oncogene exhibit defects in lymphocyte proliferation, humoral immunity, and interleukin-2 expression. *Genes and Development* 1995; **9**:1965-77.

25. Ma L, Chan KW, Trendell-Smith NJ, Wu A, Tian L, Lam AC, et al. Systemic autoimmune disease induced by dendritic cells that have captured necrotic but not apoptotic cells in susceptible mouse strains. *Eur J Immunol* 2005; **35(11)**:3364-75.

26. Werfel T. The role of leukocytes, keratinocytes, and allergen-specific IgE in the development of atopic dermatitis. *J Invest Dermatol* 2009; **129(8)**:1878-91.

27. Fyhrquist N, Lehtimaki S, Lahl K, Savinko T, Lappetelainen AM, Sparwasser T, et al. Foxp3+ cells control Th2 responses in a murine model of atopic dermatitis. *J Invest Dermatol* 2012; **132(6)**:1672-80.

28. Isomura I, Palmer S, Grumont RJ, Bunting K, Hoyne G, Wilkinson N, et al. c-Rel is required for the development of thymic Foxp3+ CD4 regulatory T cells. *J Exp Med* 2009; **206(13)**:3001-14.

29. Mathis D, Benoist C. Aire. *Annu Rev Immunol* 2009; **27**:287-312.

30. Gray DH, Gavanescu I, Benoist C, Mathis D. Danger-free autoimmune disease in Aire-deficient mice. *Proceedings of the National Academy of Sciences of the United States of America* 2007; **104(46)**:18193-8.

31. Gerondakis S, Fulford TS, Messina NL, Grumont RJ. NF-kappaB control of T cell development. *Nat Immunol* 2014; **15(1)**:15-25.

32. Irla M, Hollander G, Reith W. Control of central self-tolerance induction by autoreactive CD4(+) thymocytes. *Trends Immunol* 2010; **31(2)**:71-9.

33. Flammer JR, Rogatsky I. Minireview: Glucocorticoids in autoimmunity: unexpected targets and mechanisms. *Mol Endocrinol* 2011; **25(7)**:1075-86.

34. Strnad J, Burke JR. IkappaB kinase inhibitors for treating autoimmune and inflammatory disorders: potential and challenges. *Trends Pharmacol Sci* 2007; **28(3)**:142-8.

35. Kalergis AM, Iruretagoyena MI, Barrientos MJ, Gonzalez PA, Herrada AA, Leiva ED, et al. Modulation of nuclear factor-kappaB activity can influence the susceptibility to systemic lupus erythematosus. *Immunology* 2009; **128(1 Suppl)**:e306-14.

36. Vallabhapurapu S, Ryseck RP, Malewicz M, Weih DS, Weih F. Inhibition of NF-κB in T cells blocks lymphoproliferation and partially rescues autoimmune disease in *gld/gld* mice. *Eur J Immunol* 2001; **31(9)**:2612-22.

37. Ishimaru N, Kishimoto H, Hayashi Y, Sprent J. Regulation of naive T cell function by the NF-kappaB2 pathway. *Nat Immunol* 2006; **7**(7):763-72.

38. Siebenlist U, Brown K, Claudio E. Control of lymphocyte development by nuclear factor-kappaB. *Nat Rev Immunol* 2005; **5(6)**:435-45.

39. Chen K, Coonrod EM, Kumanovics A, Franks ZF, Durtschi JD, Margraf RL, et al. Germline mutations in NFKB2 implicate the noncanonical NF-kappaB pathway in the pathogenesis of common variable immunodeficiency. *Am J Hum Genet* 2013; **93(5)**:812-24.

40. Lee CE, Fulcher DA, Whittle B, Chand R, Fewings N, Field M, et al. Autosomal-dominant B-cell deficiency with alopecia due to a mutation in NFKB2 that results in nonprocessable p100. *Blood* 2014; **124(19)**:2964-72.
41. Lindsley AW, Qian Y, Valencia CA, Shah K, Zhang K, Assa'ad A. Combined immune deficiency in a patient with a novel NFKB2 mutation. *J Clin Immunol* 2014; **34(8)**:910-5.
42. Hao Z, Hampel B, Yagita H, Rajewsky K. T Cell-specific Ablation of Fas Leads to Fas Ligand-mediated Lymphocyte Depletion and Inflammatory Pulmonary Fibrosis. *J Exp Med* 2004; **199**:1355-65.
43. Elsharkawy AM, Oakley F, Lin F, Packham G, Mann DA, Mann J. The NF-kappaB p50:p50:HDAC-1 repressor complex orchestrates transcriptional inhibition of multiple pro-inflammatory genes. *J Hepatol* 2010; **53(3)**:519-27.
44. Duan W, Wang E, Zhang F, Wang T, You X, Qiao B. Association between the NFKB1-94ins/del ATTG polymorphism and cancer risk: an updated meta-analysis. *Cancer Invest* 2014; **32(7)**:311-20.
45. Strasser A, Grumont RJ, Stanley ML, Gerondakis S. The transcriptional regulator Rel is essential for antigen receptor-mediated stimulation of mature T cells but dispensable for positive and negative selection of thymocytes and T cell apoptosis. *Eur J Immunol* 1999; **29(3)**:928-35.
46. Chen G, Hardy K, Pagler E, Ma L, Lee S, Gerondakis S, et al. The NF-kappaB transcription factor c-Rel is required for Th17 effector cell development in experimental autoimmune encephalomyelitis. *J Immunol* 2011; **187(9)**:4483-91.
47. Gilmore TD, Gerondakis S. The c-Rel Transcription Factor in Development and Disease. *Genes Cancer* 2011; **2(7)**:695-711.
48. Liu FT, Goodarzi H, Chen HY. IgE, mast cells, and eosinophils in atopic dermatitis. *Clin Rev Allergy Immunol* 2011; **41(3)**:298-310.

49. Matsuda H, Watanabe N, Geba GP, Sperl J, Tsudzuki M, Hiroi J, et al. Development of atopic dermatitis-like skin lesion with IgE hyperproduction in NC/Nga mice. *Int Immunol* 1997; **9(3)**:461-6.

50. Zelazowski P, Shen Y, Snapper CM. NF-kappaB/p50 and NF-kappaB/c-Rel differentially regulate the activity of the 3'alphaE-hsl,2 enhancer in normal murine B cells in an activation-dependent manner. *Int Immunol* 2000; **12(8)**:1167-72.

51. Freyschmidt EJ, Mathias CB, Diaz N, MacArthur DH, Laouar A, Manjunath N, et al. Skin inflammation arising from cutaneous regulatory T cell deficiency leads to impaired viral immune responses. *J Immunol* 2010; **185(2)**:1295-302.

52. Shono Y, Tuckett AZ, Ouk S, Liou HC, Altan-Bonnet G, Tsai JJ, et al. A small-molecule c-Rel inhibitor reduces alloactivation of T cells without compromising antitumor activity. *Cancer discovery* 2014; **4(5)**:578-91.

FIGURE LEGENDS

Figure 1 Loss of c-REL prolongs the lifespan of *Fas*$^{lpr/lpr}$ mice whereas loss of NF-κB1 or NF-κB2 caused only modest extension of lifespan. (**a**) Kaplan-Meyer survival curves for wt (median survival 860 days, n=57, blue line), *Fas*$^{lpr/lpr}$ (n=64, median survival 402 days, red line), *nfkb1*$^{-/-}$ (n=97, median survival 614 days, dotted purple line), *nfkb2*$^{-/-}$ (n=55, median survival 755 days, dotted black line), *c-rel*$^{-/-}$ (n=54, median survival 888 days, dotted green line), *Fas*$^{lpr/lpr}$*nfkb1*$^{-/-}$ (n=65, median survival 449 days, purple line), *Fas*$^{lpr/lpr}$*nfkb2*$^{-/-}$ (n=42, median survival 445 days, solid black line), and *Fas*$^{lpr/lpr}$*c-rel*$^{-/-}$ (n=44, median survival 685 days, solid green line) mice (wt *vs* *Fas*$^{lpr/lpr}$: p<0.0001; *Fas*$^{lpr/lpr}$ *vs* *Fas*$^{lpr/lpr}$*nfkb1*$^{-/-}$: p=0.0068; *Fas*$^{lpr/lpr}$ *vs* *Fas*$^{lpr/lpr}$*nfkb2*$^{-/-}$: p=0.0218; *Fas*$^{lpr/lpr}$ *vs* *Fas*$^{lpr/lpr}$*c-rel*$^{-/-}$: p<0.0001, wt *vs* *nfkb2*$^{-/-}$: p=0.0292, wt *vs* c-*rel*$^{-/-}$: p=ns). Data are from current and historical cohorts. (**b**) Representative confocal photomicrographs of frozen sections (8 kidneys/genotype analysed) stained for the presence of IgM-, IgG- or IgA-containing immune complex deposits (green) in glomeruli. Nuclei are revealed by staining with DAPI (blue). Arrows indicate immune complex deposition on the glomerular basement membrane (scale bars represent 23.8 μm). (**c**) Kaplan-Meyer curves representing the incidence of severe autoimmune kidney disease (glomerulonephritis (GN) score ≥2 for mice of the indicated genotypes (*Fas*$^{lpr/lpr}$ *vs* *Fas*$^{lpr/lpr}$*nfkb1*$^{-/-}$: p=ns, *Fas*$^{lpr/lpr}$ *vs* *Fas*$^{lpr/lpr}$*nfkb2*$^{-/-}$: p=ns, *Fas*$^{lpr/lpr}$ *vs* *Fas*$^{lpr/lpr}$*c-rel*$^{-/-}$: p=0.0019, lines colored as for (**a**))). Data are from current and historical cohorts. (**d**) Representative H&E stained sections of kidneys from mice of the indicated genotypes were examined for pathological changes, such as glomerular hyper-cellularity, leukocyte infiltration, thickening of glomerular capillaries, cellular crescents, interstitial inflammationdilated tubules or sclerotic glomeruli. Number in brackets indicates clinical GN score; arrows indicate inflammatory infiltration; asterisk indicates protein deposition (immune complex deposits). Magnification x40.

Figure 2 Impact of loss of NF-κB1, NF-κB2 or c-REL on the serum levels of pro-inflammatory cytokines and chemokines in *Fas*$^{lpr/lpr}$ mice. The levels of 23 cytokines and chemokines (indicated in the Methods section) were measured in the sera of mice of the indicated genotypes by the Multiplex system at 5 months and when animals were terminally ill or aged. The levels of IL-1β, IL-5, IL-6, IL-17F, IFN-γ, TNF-α, MIP−1β, MCP-1, Eotaxin and IL-12 are shown. Each dot represents a single mouse; the bar indicates the average +/-SEM. Statistical analysis was performed by Mann Whitney U test; * p<0.05, ** p<0.01, *** p<0.005.

Figure 3 Loss of NF-κB2 accelerated and increased the magnitude of lymphadenopathy and splenomegaly in *Fas*$^{lpr/lpr}$ mice and loss of NF-κB1, NF-κB2 or c-REL all reduced hyper-gammaglobulinaemia and ANA levels in the serum of *Fas*$^{lpr/lpr}$ mice. (**a**) Weights of lymph nodes (axillary, brachial, inguinal and mesenteric) and spleens from mice of the indicated genotypes at the ages indicated. (**b**) The percentages of the 'unusual' TCRα/β^{+}CD3^{+}CD4^{-}CD8^{-}B220^{+} (DN) T lymphoid cells in the lymph nodes of mice of the indicated genotypes were measured by FACS analysis. In (**a**) and (**b**) each dot represents a single mouse and the figure legend depicted in (**b**) also applies to (**a**). (**c**) Graph showing total cell numbers for the indicated organs of mice of the indicated genotypes at 5 months of age (n=3-4 mice per genotype). (**d**) The levels of antibodies of the different Ig isotypes in the sera of mice of the indicated genotypes (age 5 months) are shown. Data represent mean +/- SEM (n = 6 mice per genotype). (**e**) Pictorial examples of ANA quantification by staining of human HEp-2 epithelial cells after staining with sera of mice of the indicated genotypes are shown (immunofluorescence intensity score is indicated in brackets). Positive control sera were from sick *Fas*$^{gld/gld}$ mutant mice. (**f**) Quantification of ANA staining from experiments shown in (**e**) according to fluorescence intensity on a scale of 0: no fluorescence to 3+: maximal fluorescence. (**g**) Graphical representation of the measurements of ANA levels in sera of mice of the indicated genotypes as quantified by ELISA (n = 6 mice per genotype). Values in graphs represent mean +/-SEM. Statistical analysis was performed by t-test with unequal variances; * $p<0.05$, ** $p<0.01$, *** $p<0.005$, **** $p<0.0005$.

Figure 4 *Fas*$^{lpr/lpr}$*nfkb2*$^{-/-}$ mice develop more severe lymphoproliferative disease than *Fas*$^{lpr/lpr}$ mice. (**a**) Representative photomicrographs of lung, liver and salivary glands from mice of the indicated genotypes (5 months); arrows indicate areas of lymphocyte infiltration, n=3-4 mice per genotype. (**b**) Summary (mean +/-SEM) of the incidence of lymphocytic infiltration into the indicated organs of mice of the indicated genotypes (5 months of age), graded 0-3+, n=3-4 mice per genotype. (**c**) Representative images, depicting autoimmune dermatitis in mice of the indicated genotypes. (**d**) Serum IgE levels measured by ELISA when the animals were afflicted with dermatitis or otherwise sick, n=6 mice per genotype, except *Fas*$^{lpr/lpr}$*c-rel*$^{-/-}$ mice (n=16). Values in graphs represent mean +/-SEM. Statistical analysis was performed by one way ANOVA test; **** $p<0.0005$.

Figure 5 $CD4^+CD25^+Foxp3^+$ T regulatory cells are not a limiting factor in the autoimmune disease of $Fas^{lpr/lpr}$ mice. (**a**) The percentages of T_{reg} cells ($CD4^+CD25^+Foxp3^+$) in the thymus, spleen and lymph nodes of mice of the indicated genotypes at 6, 12 and 20 weeks of age were determined by flow cytometric analysis. Each dot represents a single mouse (n=3-4 per genotype); bars indicate the average. (**b**) Absolute numbers of T_{reg} cells ($CD4^+CD25^+Foxp3^+$) in mice of the indicated genotypes as determined by flow cytometric analysis (n=3-4 per genotype at 20 weeks of age). The legend depicted in (**b**) also applies to (**a**). Data are presented as means +/-SEM. Statistical analysis was performed by t-test with unequal variances; * $p<0.05$, ** $p<0.01$, *** $p<0.005$, **** $p<0.0005$.

Figure 6 $Fas^{lpr/lpr}$ mice have no abnormalities in mTEC numbers or AIRE expression, but loss of NF-κB2 causes abnormalities in the thymic stroma. (**a**) Representative confocal images of thymi from mice of the indicated genotypes at 6 weeks and (**b**) at 20 weeks. Sections were stained for UEA-1 (green), AIRE (red) and keratin-5 (blue), n=3 mice per genotype per time point. (**c**) Graphical representation of total numbers of TEC subsets in the thymi from mice of the indicated genotypes at 20 weeks of age. TEC subsets were as defined: $mTEC^{hi}$ ($CD45^-$ Ep-CAM^+ class II MHC^{hi} $Ly51^-$), $mTEC^{low}$ ($CD45^-$ Ep-CAM^+ class II MHC^{low} $Ly51^-$), cTEC ($CD45^-$ Ep-CAM^+ class II MHC^+ $Ly51^+$); n=3-4 mice per genotype. (**d**) Graphical depiction of the numbers and percentages of $mTEC^{hi}AIRE^+$ mTECS ($CD45^-$ Ep-CAM^+ class II MHC^{hi} $Ly51^-$ $AIRE^+$) in mice of the indicated genotypes at 20 weeks of age as determined by flow cytometric analysis$^+$); n=3-4 mice per genotype. Data are presented as means +/-SEM. Statistical analysis was performed by t-test with unequal variances; * $p<0.05$, ** $p<0.01$, *** $p<0.005$, **** $p<0.0005$.

TABLE LEGENDS

Table 1 Percentages of mice of the indicated genotypes containing organ-specific autoantibodies against the tissues indicated.

Table 2 Summary of the effects of loss of NF-κB2, NF-κB2 or c-REL on the phenotype of $Fas^{lpr/lpr}$ mice.

Figure 1

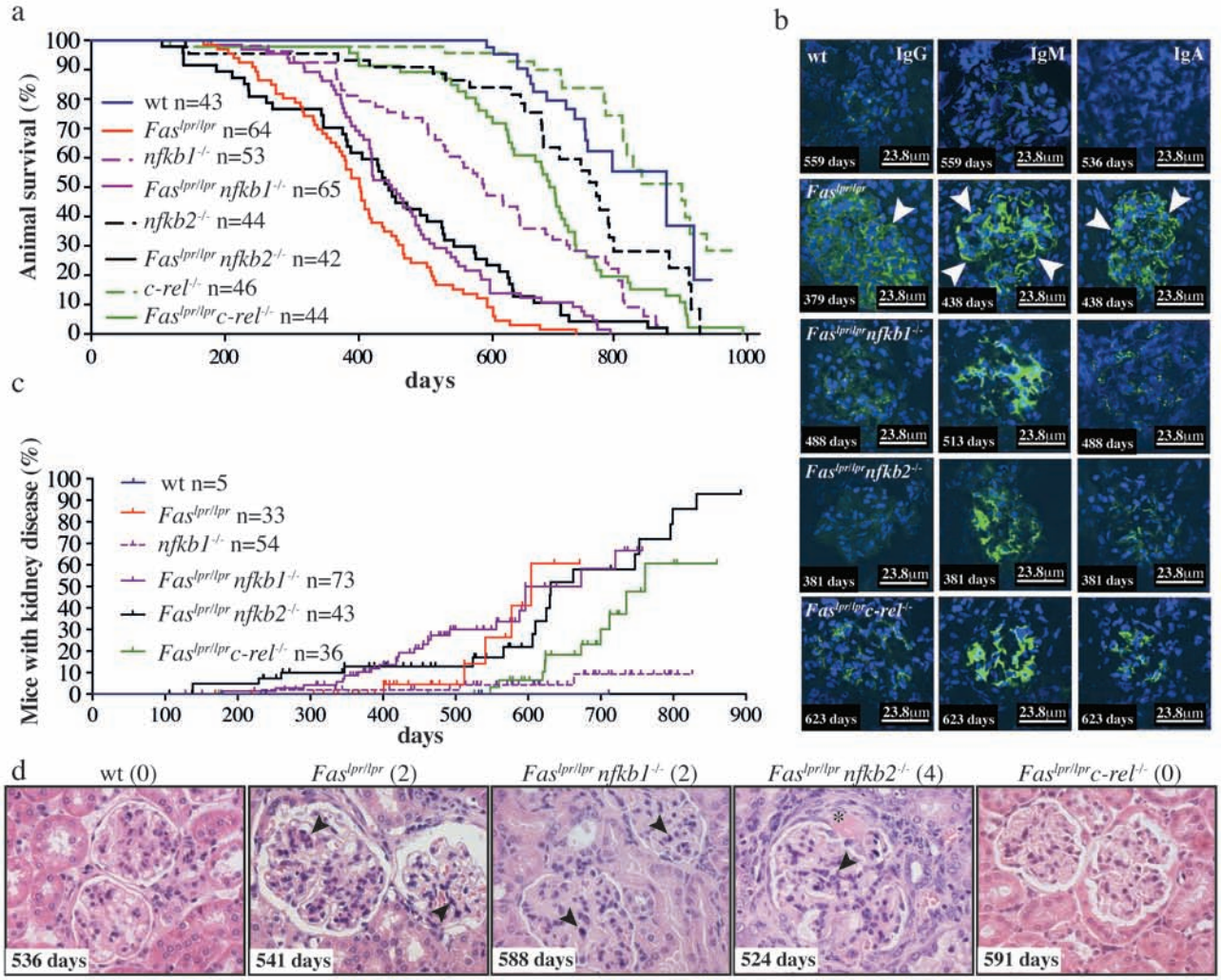
a
Animal survival (%)
wt n=43
Fas^lpr/lpr n=64
nfkb1^-/- n=53
Fas^lpr/lpr nfkb1^-/- n=65
nfkb2^-/- n=44
Fas^lpr/lpr nfkb2^-/- n=42
c-rel^-/- n=46
Fas^lpr/lpr c-rel^-/- n=44
days
b
wt
IgG
IgM
IgA
559 days
559 days
536 days
Fas^lpr/lpr
379 days
438 days
438 days
Fas^lpr/lpr nfkb1^-/-
488 days
513 days
488 days
Fas^lpr/lpr nfkb2^-/-
381 days
381 days
381 days
Fas^lpr/lpr c-rel^-/-
623 days
623 days
623 days
23.8µm
c
Mice with kidney disease (%)
wt n=5
Fas^lpr/lpr n=33
nfkb1^-/- n=54
Fas^lpr/lpr nfkb1^-/- n=73
Fas^lpr/lpr nfkb2^-/- n=43
Fas^lpr/lpr c-rel^-/- n=36
days
d
wt (0)
Fas^lpr/lpr (2)
Fas^lpr/lpr nfkb1^-/- (2)
Fas^lpr/lpr nfkb2^-/- (4)
Fas^lpr/lpr c-rel^-/- (0)
536 days
541 days
588 days
524 days
591 days

Figure 2

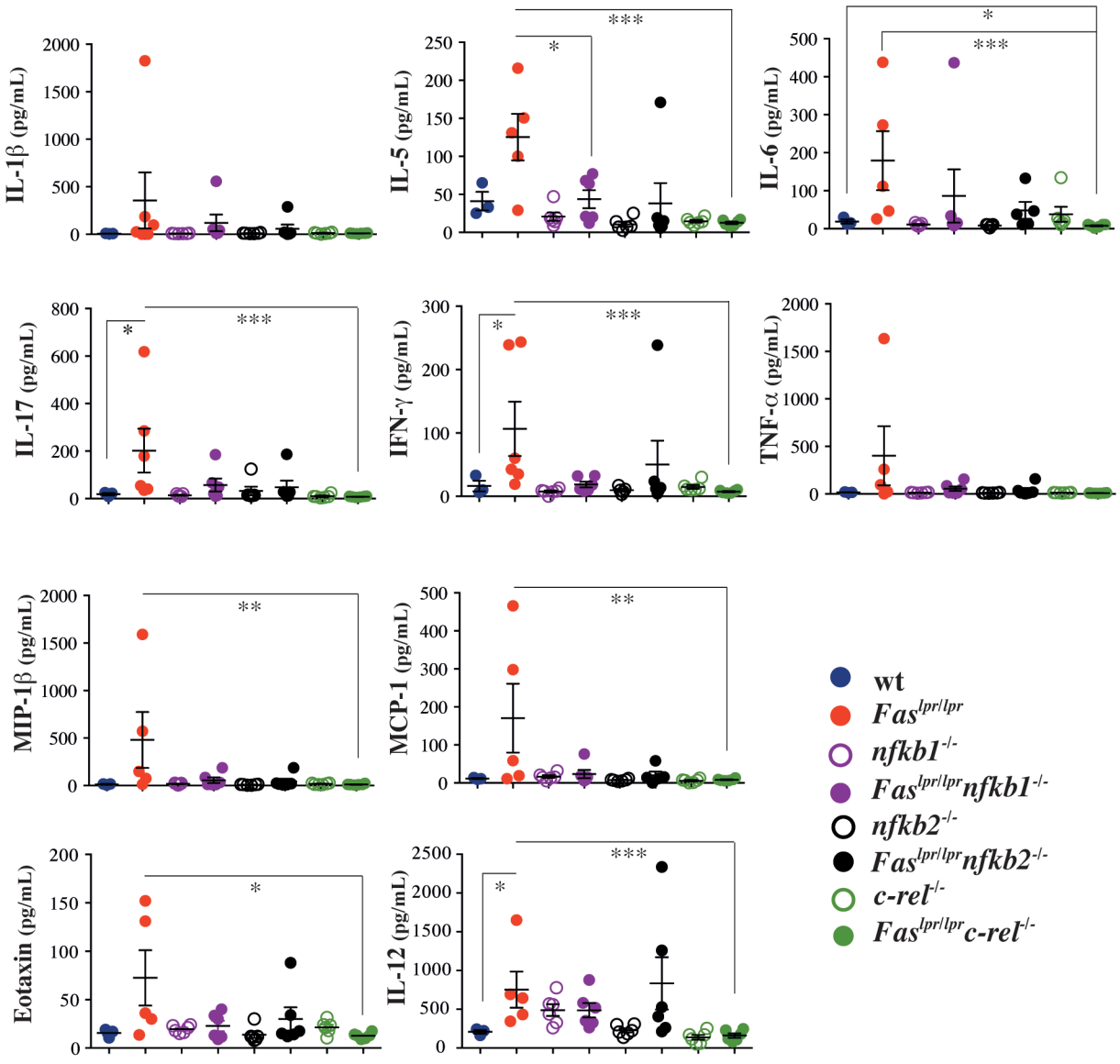
IL-1β (pg/mL)
IL-5 (pg/mL)
IL-6 (pg/mL)
IL-17 (pg/mL)
IFN-γ (pg/mL)
TNF-α (pg/mL)
MIP-1β (pg/mL)
MCP-1 (pg/mL)
Eotaxin (pg/mL)
IL-12 (pg/mL)
wt
Fas^lpr/lpr
nfkb1^-/-
Fas^lpr/lpr nfkb1^-/-
nfkb2^-/-
Fas^lpr/lpr nfkb2^-/-
c-rel^-/-
Fas^lpr/lpr c-rel^-/-

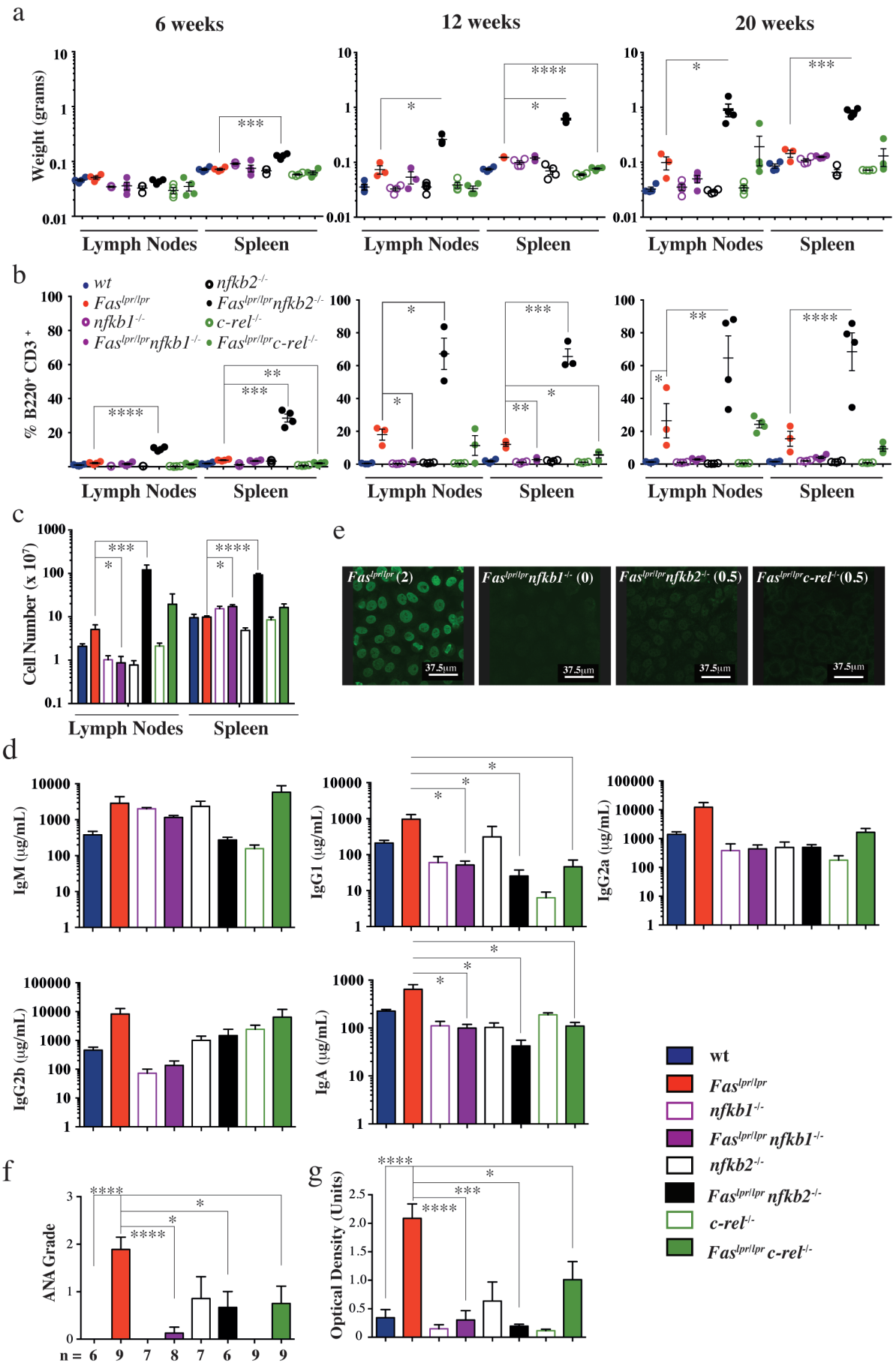
a
6 weeks
12 weeks
20 weeks
Weight (grams)
Lymph Nodes
Spleen
b
wt
Fas lpr/lpr
nfkb1 -/-
Fas lpr/lpr nfkb1 -/-
nfkb2 -/-
Fas lpr/lpr nfkb2 -/-
c-rel -/-
Fas lpr/lpr c-rel -/-
% B220+ CD3+
c
Cell Number (x 10^7)
e
Fas lpr/lpr (2)
Fas lpr/lpr nfkb1 -/- (0)
Fas lpr/lpr nfkb2 -/- (0.5)
Fas lpr/lpr c-rel -/- (0.5)
37.5µm
d
IgM (µg/mL)
IgG1 (µg/mL)
IgG2a (µg/mL)
IgG2b (µg/mL)
IgA (µg/mL)
wt
Fas lpr/lpr
nfkb1 -/-
Fas lpr/lpr nfkb1 -/-
nfkb2 -/-
Fas lpr/lpr nfkb2 -/-
c-rel -/-
Fas lpr/lpr c-rel -/-
f
ANA Grade
n = 6 9 7 8 7 6 9 9
g
Optical Density (Units)

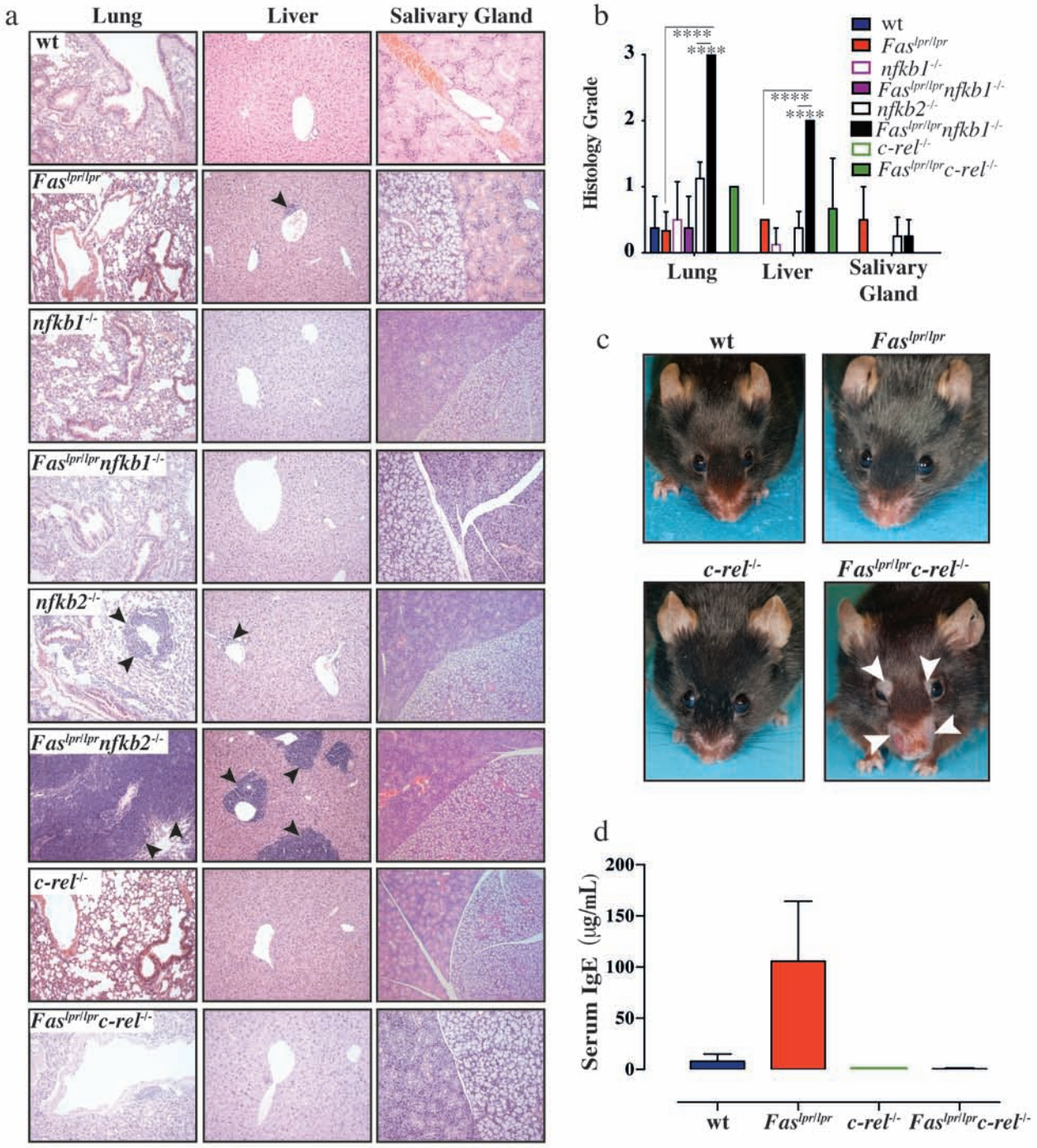
a
Lung
Liver
Salivary Gland
wt
Fas lpr/lpr
nfkb1 -/-
Fas lpr/lpr nfkb1 -/-
nfkb2 -/-
Fas lpr/lpr nfkb2 -/-
c-rel -/-
Fas lpr/lpr c-rel -/-
b
Histology Grade
0
1
2
3
****
****
****
****
Lung
Liver
Salivary Gland
wt
Fas lpr/lpr
nfkb1 -/-
Fas lpr/lpr nfkb1 -/-
nfkb2 -/-
Fas lpr/lpr nfkb1 -/-
c-rel -/-
Fas lpr/lpr c-rel -/-
c
wt
Fas lpr/lpr
c-rel -/-
Fas lpr/lpr c-rel -/-
d
Serum IgE (µg/mL)
0
50
100
150
200
wt
Fas lpr/lpr
c-rel -/-
Fas lpr/lpr c-rel -/-

Figure 5

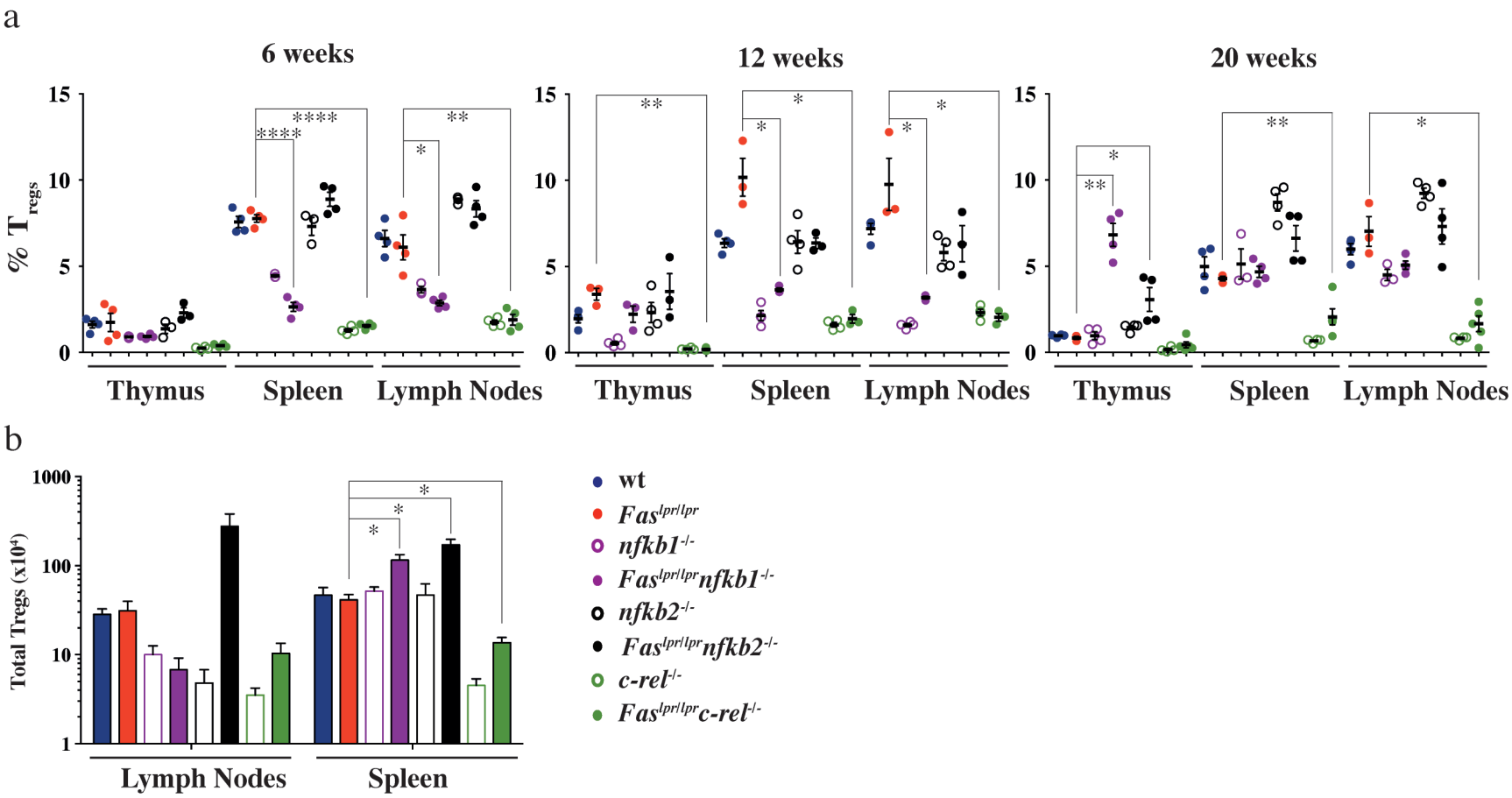
a
6 weeks
12 weeks
20 weeks
% T regs
15
10
5
0
Thymus
Spleen
Lymph Nodes
b
Total Tregs (x10⁴)
1000
100
10
1
Lymph Nodes
Spleen
wt
Faslpr/lpr
nfkb1-/-
Faslpr/lprnfkb1-/-
nfkb2-/-
Faslpr/lprnfkb2-/-
c-rel-/-
Faslpr/lprc-rel-/-

Figure 6

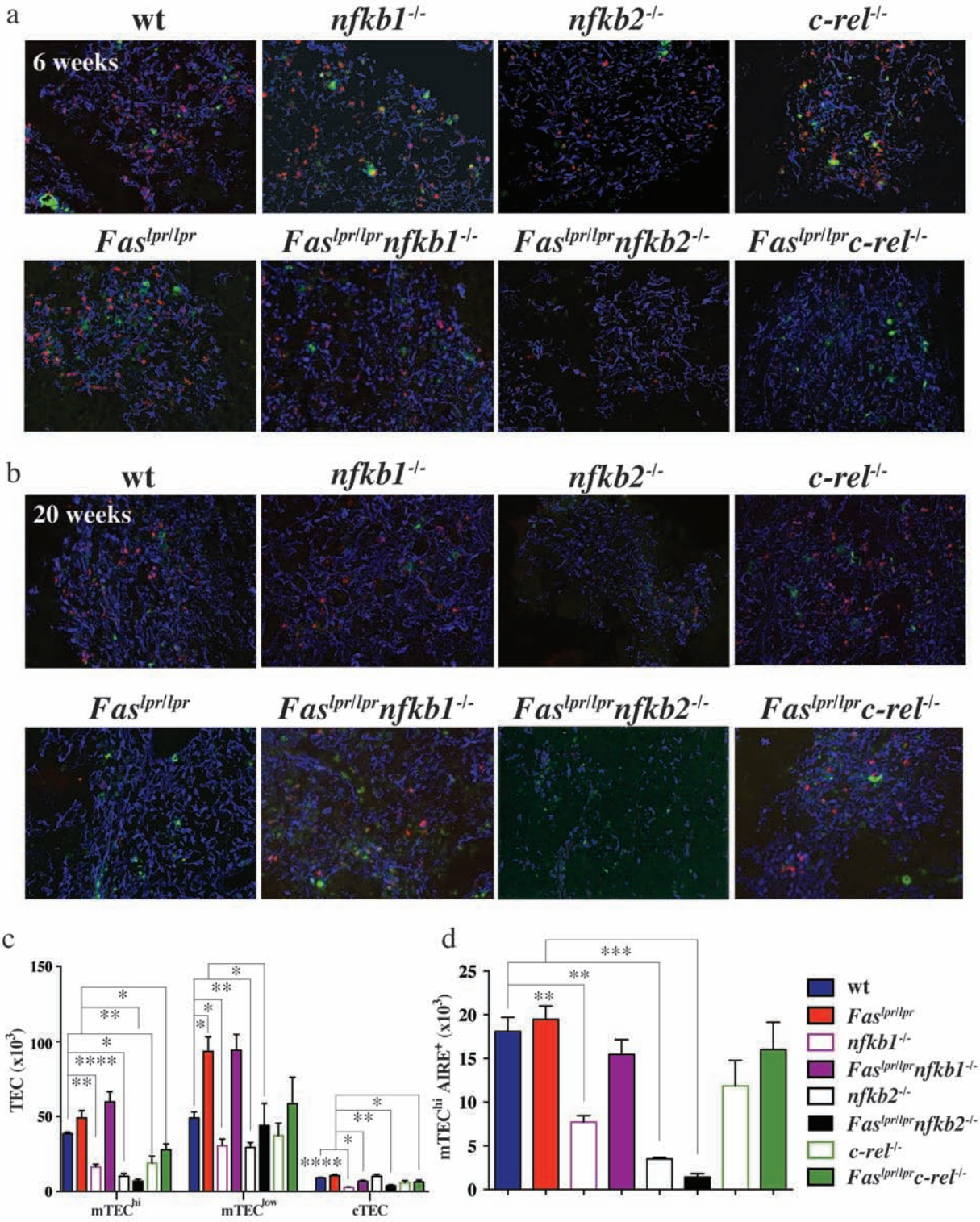
a
wt
nfkb1-/-
nfkb2-/-
c-rel-/-
6 weeks
Fas lpr/lpr
Fas lpr/lpr nfkb1-/-
Fas lpr/lpr nfkb2-/-
Fas lpr/lpr c-rel-/-
b
wt
nfkb1-/-
nfkb2-/-
c-rel-/-
20 weeks
Fas lpr/lpr
Fas lpr/lpr nfkb1-/-
Fas lpr/lpr nfkb2-/-
Fas lpr/lpr c-rel-/-
c
TEC (x10^3)
150
100
50
0
mTEC hi
mTEC low
cTEC
d
mTEC hi AIRE+ (x10^3)
25
20
15
10
5
0
wt
Fas lpr/lpr
nfkb1-/-
Fas lpr/lpr nfkb1-/-
nfkb2-/-
Fas lpr/lpr nfkb2-/-
c-rel-/-
Fas lpr/lpr c-rel-/-